Biochemical Engineering Journal 177 (2022) 108224

Contents lists available at ScienceDirect

Biochemical Engineering Journal

journal homepage: www.elsevier.com/locate/bej

Determination of culture design spaces in shaken disposable cultivation systems for CHO suspension cell cultures

Rüdiger W. Maschke [a,b,*], Stefan Seidel [a], Thomas Bley [b], Regine Eibl [a], Dieter Eibl [a]

[a] Zurich University of Applied Sciences, School of Life Sciences and Facility Management, Institute of Chemistry and Biotechnology, Grüentalstrasse 14, 8820, Wädenswil, Switzerland

[b] Technische Universität Dresden, Institute of Natural Materials Technology, Bioprocess Engineering, Bergstrasse 120, 01069, Dresden, Germany

ARTICLE INFO

Keywords:
Erlenmeyer shake flask
Optimum Growth flask
TubeSpin bioreactor
CHO suspension cell culture
Process engineering characterization
Design space

ABSTRACT

Processes involving mammalian cell cultures - especially CHO suspension cells - dominate biopharmaceutical manufacturing. These processes are usually developed in small scale orbitally shaken cultivation systems, and thoroughly characterizing these cultivation systems is crucial to their application in research and the subsequent scale-up to production processes. With the knowledge of process engineering parameters such as oxygen transfer rate, mixing time, and power input, in combination with the demands set by the biological production system, biomass growth and product yields can be anticipated and even increased. However, the available data sources for orbitally shaken cultivation systems are often incomplete and thus not sufficient enough to generate suitable cultivation requirements. Furthermore, process engineering knowledge is inapplicable if it is not linked to the physiological demands of the cells.

In the current study, a simple yet comprehensive approach for the characterization and design space prediction of orbitally shaken single-use cultivation systems is presented, including the "classical" Erlenmeyer shake flask, the cylindrical TubeSpin bioreactor and the alternately designed Optimum Growth flask. Cultivations were performed inside and outside the design space to validate the defined culture conditions, so that cultivation success (desired specific growth rates and viable cell densities) could be achieved for each cultivation system.

1. Introduction

The steadily growing biopharmaceuticals market is dominated by products produced from mammalian cell cultures, and this approach is used by more than three quarters of biopharmaceutical manufacturers [1]. Currently, the primary driver for the development of new processes is through the use of Chinese hamster ovary (CHO) cells, from which monoclonal antibodies for therapeutic use and biosimilars are produced [1]. In most cases, studies investigating these new processes are carried out in small orbital shaken cultivation systems, such as multiwell plates, tubes, and shake flasks, allowing for cost-effective and efficient parallelized screening. The most widely used and best characterized orbital shaken cultivation system is the Erlenmeyer flask, which was developed by Emil Erlenmeyer in the 19th century and named after him years later [2,3]. Since, the material that is used, as well as the design of the Erlenmeyer flask, has undergone a number of adaptations. There are, for example, versions with narrow and wide necks, and with or without baffles. A wide variety of sterile barriers are also available [4]. Especially for CHO cells, unbaffled single-use Erlenmeyer flasks have proven to be the best option, as they reduce the likelihood of (cross-)contamination and preparation time. Since the basic geometric shape of unbaffled Erlenmeyer flasks causes the surface area of its contents to consistently decline as volume increases, this tapering can restrict the exchange of oxygen. As a result of this, the filling volume of CHO cell cultures in Erlenmeyer flasks is usually restricted to less than 40% of the nominal volume. In order to ensure a sufficiently large surface area at filling volumes over 40%, alternative geometries have been developed, such as the TubeSpin bioreactor [5–7] from TPP - Techno Plastic Products AG, which is based on centrifuge tubes, or the Optimum Growth flask [8,9] from Thomson Instrument Company, which increases the surface area and thus the filling volume through a higher angle of inclination compared to the conventional Erlenmeyer flask. However, it should be noted that the surface-to-volume ratio of TubeSpin bioreactors and Thomson flasks also decreases as the filling volume increases. This

* Corresponding author at: Zurich University of Applied Sciences, School of Life Sciences and Facility Management, Institute of Chemistry and Biotechnology, Grüentalstrasse 14, 8820, Wädenswil, Switzerland.
E-mail address: ruediger.maschke@zhaw.ch (R.W. Maschke).

https://doi.org/10.1016/j.bej.2021.108224
Received 8 June 2021; Received in revised form 27 September 2021; Accepted 29 September 2021
Available online 2 October 2021

leads to a reduced specific interfacial area and consequently to a decrease in the oxygen transfer rate [10]. In addition, small scale stirred bioreactor systems have emerged, easing the challenges associated with scaling up and down.

Considering these alternatives, why should processes in orbitally shaken cultivation systems be further developed? Well, in tandem with the advantages of low price and effort, an understanding of the process engineering characteristics of shaken cultivation systems can allow for the investigation of the potential limiting factors of a cell line-medium combination. This knowledge can be utilized to multiparametrically determine the technical limitations of a bioprocess, allowing for process transfer/scale-up within a given design space, whereby the design space predicts cultivation success with a certain failure probability. The design space, which is described as a concept in the International Council for Harmonisation of Technical Requirements for Pharmaceuticals for Human Use (ICH) Q8 guideline, is a hypercube in which all factor combinations (e.g. shaking rate, filling volume, shaking diameter) can be applied without affecting the response specification (e.g. mixing time, specific power input). ICH defines the design space as "the multidimensional combination and interaction of input variables (e.g. material attributes) and process parameters that have been demonstrated to provide assurance of quality" [11]. Design spaces are increasingly used in the pharmaceutical industry as a tool for Quality by Design (QbD) [12]. QbD aims to meet customer demands consistently and efficiently. In contrast to Quality by Testing, QbD aims to build quality into the process, and ultimately the final product, during its development [13]. The above mentioned definition of a design space is exemplified by Abu-Absi et al. through the example of a CHO based monoclonal antibody production process [14]. In this study, the authors were able to determine critical process parameters in a scale-down model by varying process (e.g. dissolved oxygen, pH, agitation rate) and cell physiological (e.g. inital viable cell density, temperature shift) parameters [14].

The definition of a design space is based on the regression models

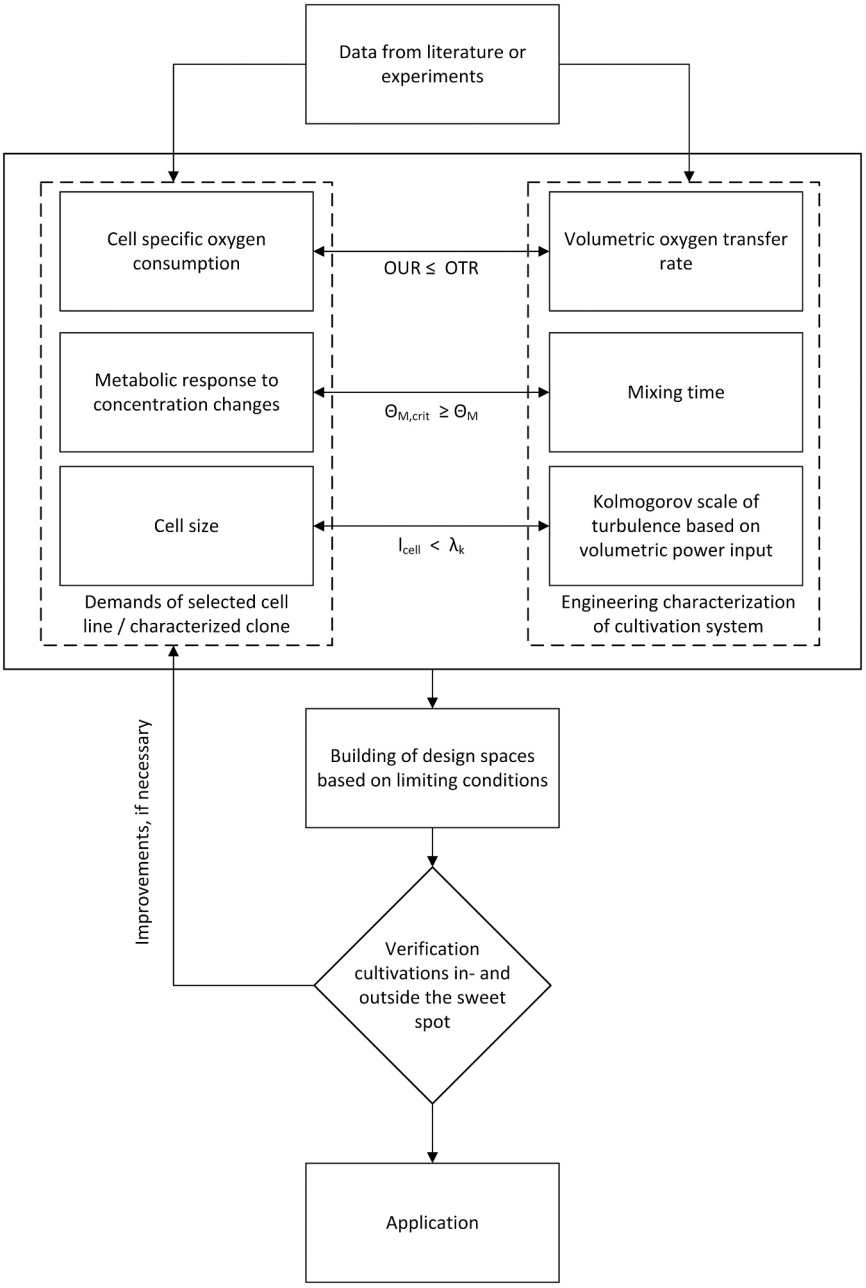

Fig. 1. Workflow for creating process engineering based cell culture design spaces. Suitable data from the literature and experiments are required to determine the demands of the biological system (combination of cell line and medium, left side) as well as the capabilities of the cultivation system being investigated (right side). Both must be connected and aligned with each other in order to determine critical and limiting process conditions. Here, a comparison is made between the oxygen uptake rate (OUR) of the suspension culture and the oxygen transfer rate (OTR) of the system (subsection 2.4), the critical mixing time at which metabolic changes in the cell culture can be expected ($\Theta_{M,crit}$) with the 95% mixing time in the system (Θ_M, subsection 2.3), and the cell size (l_{cell}) with the Kolmogorov scale of micro turbulence (λ_K, subsection 2.5). Based on this data, the design space can be generated, which is subsequently verified through cultivation. If necessary, the cultivation data obtained in this way can be used to improve cell line characterization.

created and an estimate of the failure probability. For the former, a design of experiments (DoE) approach is preferably used. The probability of obtaining predictions outside the response specifications corresponds to the failure probability and can be calculated according to Kane [15]. For the development of a design space, the Monte Carlo simulation method may be used [16,17]. In this study, process engineering and cell physiological data are combined to create a culture design space for orbitally shaken cultivation systems. Using a 500 mL Erlenmeyer flask for the cultivation of a CHO cell line (CHO XM111-10), all process steps are described. First, the capacities of the cultivation system and potential limitations of the cell line are identified. Subsequently, the design space is created based on the determined data. Afterwards, cultivations are performed within and outside the selected limits, along with a process transfer to a TubeSpin and Optimum Growth flask.

2. Material and methods

2.1. General approach

The approach of this work is depicted in Fig. 1. Both literature and experimental data can be used to characterize the cell line (left side) and the cultivation system (right side), so both will be compared in the following subsections. In the case of doubt, self-obtained experimental values are to be preferred, since deviations due to modified cell lines, measurement techniques etc. can have a considerable influence. For orbitally shaken cultivation systems, three critical parameters have been defined for which the demands of the cell line can be compared with the procedural properties of the cultivation system:

- The cell specific oxygen demand and thus the oxygen uptake rate (OUR) must be matched by the oxygen transport capabilities of the cultivation system (oxygen transfer rate OTR).
- A metabolic response to substrate limitation, accumulation of inhibiting metabolites or pH-gradients has to be avoided and thus, a sufficient degree of uniformity must be guaranteed.
- Cell damage or growth reduction caused by fluid mechanical stress has to be avoided. This can be achieved by predicting the minimal eddy size by means of volumetric power input calculation and thus ensure eddy sizes greater than the cell sizes.

Fig. 2. Depiction of the investigated disposable orbitally shaken cultivation systems. From left to right: 50 and 600 mL TubeSpin (made of polypropylene), 500 mL Erlenmeyer flask (made of polycarbonate), 500 and 5000 mL Optimum Growth flask (made of polypropylene).

With all the data gathered, a design space can be created which depicts the risk of not meeting the selected criteria. Cultivations can then be performed at presumably favorable and unfavorable conditions to verify the concept in one cultivation system. Experiments can be assessed in different ways, such as by evaluating biomass growth over maximum specific growth rate and maximum cell density or productivity over product quality and quantity. To reduce the effects of media variation and ensure comparability with other studies, the maximum specific growth rate μ_{max} is used as the main comparison criterion for evaluating the process engineering effects [18]. In the case of significant deviations, the assumptions made (especially on the cell line characterization side) have to be reviewed. Otherwise, the concept can be transferred to other process engineering characterized cultivation systems.

However, it must be noted that various factors besides the process engineering settings can limit growth and product formation in a biotechnological process [19]. Therefore, to evaluate the influence of process engineering parameters on cultivation success, variations resulting from media and inoculum preparation must be avoided. The following sections describe how characteristics of the engineering and cell line data were determined and design spaces were created.

2.2. Investigation space

All of the examined cultivation systems are depicted in Fig. 2. The investigation space that was utilized for the 50 mL TubeSpin (TS50), the 500 mL Erlenmeyer flask (EF500), the 500 mL Optimum Growth flask (OG500), the 600 mL TubeSpin (TS600) and the 5000 mL Optimum Growth flask (OG5000) is summarized in Table 1. All process engineering characterizations and cultivations were set within these limits. The selected attributes (filling volume, shaking rate, and shaking diameter) all had a significant influence on the investigated engineering parameters. The chosen limits were based on frequently used literature values, except for the maximum shaking rate, which was set higher to investigate the shear sensitivity of the cells. The distribution of individual measuring points in the process engineering characterization design space was realized via a central composite face centered (CCF) DoE approach. A central composite design was chosen because it produces similar results to full factorial designs with a reduced number of experiments [20]. The CCF solution is a compromise: a larger process space is covered compared to a central composite inscribed (CCI) design, while at the same time all experiments are conducted within the technical limits (for example, the maximum shaking rate), which are exceeded using a broader central composite circumscribed (CCC) design [21]. Using the DoE software MODDE 12 (Sartorius AG, Göttingen, Germany), models were created to interpolate the mixing time, k_La, and power input values between the measuring points.

Table 1
Experimental space of investigations as well as geometric and material properties of the investigated orbitally shaken cultivation systems.

Parameter	Symbol	EF500	TS50	TS600	OG500	OG5000
Material		Polycarbonate		Polypropylene		
Geometric parameters						
Total volume [mL]	V_T	595	60	845	550	4800
Inner diameter [mm]	d_i	98	28	94	96	227
Total height [mm]	h_t	175	115	181	143	248
Selected settings						
Filling volume [mL]	V_L	50–200	10–30	200–400	100–250	1200–3000
Shaking rate [rpm]	N	80–300	110–300	110–300	80–300	70–250
Shaking diameter [mm]	d_0			25 and 50		

2.3. Mixing time

In contrast to oxygen saturation or fluid dynamic stress considerations, exact values regarding limiting respectively critical mixing times are rarely published. In general, mixing times below 30 s at laboratory scale ($\leq$ 10 L) [22] and 2 min at production scale ($\geq$ 100 L) [23] seem to be important to avoid the potential limitations of oxygen, pH, and nutrient gradients. With an unspecified CHO cell line which was exposed to an oxygen gradient, Anane et al. were able to demonstrate that a mixing time greater than 90 s resulted in a clear-cut metabolic switch [24]. Thus, when this mixing time was exceeded, lactate accumulation increased and the viable cell density was lower compared to the control process. This, however, had no effect on productivity, but it did have an impact on product purity. Xu et al. also showed that insufficient mixing and high CO_2 concentrations caused lactate accumulation [25]. However, lactate did not accumulate at lower mixing times. The effect of pH fluctuations on cell growth and product formation rates with two different CHO cell lines was investigated by Paul et al. [26]. Such pH fluctuations are expected especially in large bioreactors with high mixing times and resulted in reduced, maximum cell densities in the scale-down model. Platas Barradas et al. found the highest growth rates at lab scale at mixing times between 10 and 12 s and already detected reduced growth rates at mixing times of 20 s [18]. When considering mixing, constant suspension of the cells should be assumed, since cell sedimentation leads to insufficient mass transfer and thus to reduced growth or cell death.

Experimentally determined mixing time values for orbitally shaken cultivation systems have been published by Tan et al. [27], Rodriguez et al. [28,29], and Monteil et al. [30]. However, as the literature data was incomplete for the investigated systems, the mixing time was determined by the decolorization method [27,31,32], based on the recommendation of the DECHEMA expert group for single-use technology [33]. To accomplish this, flasks were filled with water and 5 mL L^{-1} of a 10 g L^{-1} starch (Sigma-Aldrich, St. Louis, USA) solution, together with 2 mL L^{-1} iodide/potassium iodide (Sigma-Aldrich) solution (consisting of 20 g L^{-1} iodine and 40 g L^{-1} potassium iodide), resulting in a dark blue bulk solution. The decolorization process commenced with the sudden addition of sodium thiosulfate (Sigma-Aldrich) solution (24.8 g L^{-1} sodium thiosulfate pentahydrate). The mixing time was defined as the period between the addition of the thiosulfate and the complete decolorization of the bulk solution. The decolorization times were measured manually in triplicate, at 25 °C within the designated investigation space (Table 1) in a Multitron Cell shaking incubator (Infors AG, Bottmingen, Switzerland).

2.4. Cell oxygen demand and oxygen transfer rate

A sufficient supply and avoidance of fluctuations in dissolved oxygen concentration are critical for optimal growth of CHO cell suspension cultures. Adequate oxygen supply can be achieved if the oxygen transfer rate (OTR) is greater or equal to the oxygen uptake rate (OUR). The OTR consists of the volumetric mass transfer coefficient k_La, the dissolved oxygen concentration at the gas liquid interphase $c^*_{O_2,L}$ and the measured or desired dissolved oxygen concentration in the liquid $c_{O_2,L}$. The OUR can be calculated as the product of the viable biomass concentration c_x and the cell specific oxygen uptake rate q_{O_2} (Eq. 1).

$$\begin{aligned} OTR &\geq OUR \\ k_La\cdot\left(c^*_{O_2,L} - c_{O_2,L}\right) &\geq q_{O_2}\cdot c_x \end{aligned} \quad (1)$$

The cell specific oxygen uptake rate must first be measured or obtained from suitable sources in the literature. A thorough overview of the oxygen demand of different cell lines is provided by Wagner et al. [34], and extensive summaries of different measurement methods and values are provided by Garcia-Ochoa et al. [35] and Seidel et al. [36]. A synopsis of literature q_{O_2}-values is depicted in Fig. 3. It can be seen that for CHO cells, the outliers extend over two orders of magnitude, which can be explained among other things by different clones (e.g. DG44, SSF3, K1), process modes (batch, fed-batch, perfusion) and measurement methods (e.g. by gas-phase mass balance, dynamic evaluation or dissolved oxygen concentration profile calculation). Measuring the cell specific oxygen uptake rate for an investigated CHO clone is therefore recommended.

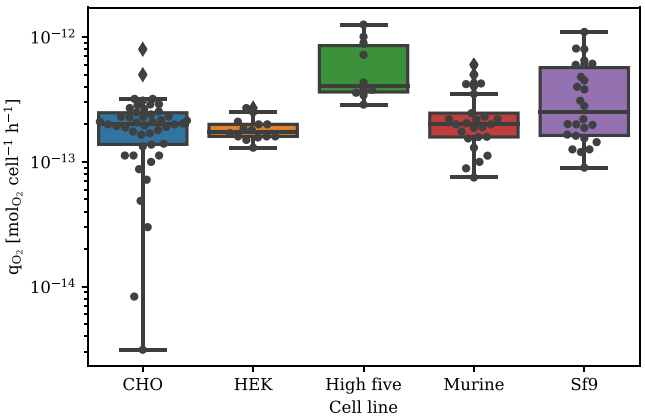

Fig. 3. Swarm-Boxplot of specific oxygen demand q_{O_2} of CHO (dark blue [37–40–43–46–49–52–55,56,57]), Human embryo kidney (HEK, orange [58–60]), *Trichoplusia ni* (High five, green [39,61,62]), Murine (red, [63–65,38,66,67,50,43,68–70]), and *Spodoptera frugiperda* (*Sf*9, violet [61,62,39,71–74–77–80]) cells.

The dependence of the volumetric mass transfer coefficient k_La from process conditions in orbitally shaken cultivation systems has been extensively investigated over the past decades. Different approaches have been summarized by Meier et al., including a new correlation for estimating the OTR in unbaffled Erlenmeyer flasks [81]. However, the oxygen transfer in shaken vessels is significantly influenced by a thin layer build of the liquid on the inside of the flask. Maier and Büchs were able to show that hydrophilic surfaces (e.g. classic glass Erlenmeyer flasks) generate higher oxygen transfer rates compared to vessels with hydrophobic surfaces (e.g. plastic flasks) [82], proving that the material should not be ignored when taking literature data into consideration. No complete data on the k_La-value could be found for the single-use systems investigated. Therefore, the determination of the k_La-values was performed according to the DECHEMA expert group recommendations for single-use technology [33], whereby the gassing-out method [83,84] was used. The dissolved oxygen concentration was measured using the shake flask reader and the selected shaken vessel with SP-PSt3-NAU oxygen sensor spots (PreSens Precision Sensing GmbH, Regensburg, Germany). The sensor spots have a response time $t_{63\%,crit}$ of approximately 14 s, which allows for the measurement of k_La-values up to 250 h^{-1} using the van't Riet criterion [85] or up to 50 h^{-1} using the more restrictive approach by Zlokarnik [86]. The cultivation system was filled to the appropriate volume with 1 x phosphate buffered saline (PBS) solution (Sigma-Aldrich) and tempered to 37°C. Afterwards, oxygen was removed from the system by gassing the bulk solution with nitrogen until a concentration of less than 5% was achieved. Then, by shaking the system, it was (passively) gassed with air until an air saturation of more than 95% was reached. The k_La-values were calculated between 10% and 90% air saturation.

2.5. Specific power input and potential of fluid dynamic stress

Several publications deal with the potential impairments of growth and product expression in CHO cell cultures due to fluid dynamic stress

(often called mechanical/shear stress) [18,87–90], but the concepts which quantify this stress vary. Often used approaches are based on the volumetric power input, the energy dissipation rate or the size of the micro-turbulence generated. Chalmers has summarized various studies with lethal and sub-lethal cell responses to mechanical stress, with lethal responses ranging from energy dissipation rates of $6 \cdot 10^6$ W m^{-3} (CHO-GS cells) to 10^8 W m^{-3} (wild type suspended CHO-K1 cells) [87]. Such a wide data range is another example of the problems associated with literature values for dramatically varying experimental conditions. Another approach utilizes the Kolmogorov scale of turbulence. Kolmogorov's microscale theory describes the formation of smaller eddies by the breakup of large scale turbulent eddies as a cascading process. At the Kolmogorov scale of turbulence, viscous and inertial forces compensate each other and the energy from the eddies dissipates [91]. Cell damage arising from the fluid dynamics is thought to occur if the micro eddies produced by the cultivation system are smaller or similar in size to the cells [90,92]. Thus, keeping the eddy size above 18 µm - the typical upper size of CHO cells - should prevent fluid dynamic damage [91].

Büchs et al. determined the power input in glass Erlenmeyer flasks with torque measurements in the shaking incubator while counterbalancing the friction losses, whereby power inputs up to 6 kW m^{-3} were measured [93]. Utilizing the power input P/V and the liquid density ρ_L, the average energy dissipation rate $\bar{\varepsilon}$ in unbaffled Erlenmeyer flasks can be calculated using Eq. 2 [94].

$$\bar{\varepsilon} = \frac{P}{V \cdot \rho_L} \tag{2}$$

In unbaffled flasks, the ratio between the average and maximum energy dissipation rate below the critical Reynolds number of 60 000 is approximately 1 and indicates non-turbulent flow [95]. For baffled shake flasks and for Reynolds numbers above 60 000, the maximum energy dissipation rate ε_{max} can be calculated analogous to stirred tanks, using the relative motion of the liquid $\pi \cdot N \cdot d_i$ (with the shaking rate N and the maximum inner diameter d_i) and the height of the liquid h_L as the characteristic length (Eq. 3) [95].

$$\varepsilon_{max} = 0.1 \cdot \frac{(\pi \cdot N \cdot d_i)^3}{h_L} \tag{3}$$

Finally, the length of the microscale λ_K can be calculated according to the Kolmogorov approach (Eq. 4), using the maximum energy dissipation rate and the kinematic viscosity of the liquid ν_L.

$$\lambda_K = \sqrt[4]{\frac{{\nu_L}^3}{\varepsilon_{max}}} \tag{4}$$

The volumetric power input was determined using computational fluid dynamics (CFD). All simulations were carried out with the open source software OpenFOAM (www.openfoam.org), version 5. The underlying simulation method was validated by Klöckner et al., where the method is described in detail [96]. The computer aided design (CAD) geometry was manually generated using Autodesk Inventor, version 2020. The number of grid cells generated was 213 297 for the 500 mL Optimum Growth flask and 824 261 cells for the 5000 mL flask, 34 804 for the 50 mL TubeSpin and 156 626 for the 600 mL TubeSpin as well as 137 452 for the 500 mL Corning Erlenmeyer flask. Physical properties were set to conditions at 25 °C, which corresponds with a water density of 997.05 kg m^{-3}, a dynamic viscosity of water of $890.02 \cdot 10^{-6}$ Pa s^{-1}, an air density of 1.17 kg m^{-3}, and a dynamic viscosity of air of $18.93 \cdot 10^{-6}$ Pa s^{-1} [97, p. 201–220]. The water-surface contact angle was set to 83° for polycarbonate (Corning) and 97° for polypropylene cultivation systems (Optimum Growth and TubeSpin) [98]. The applied transient solver interDyMFoam was used with the k-ω SST turbulence model [99]. Twenty seconds were simulated to anticipate stationary conditions. For every shaking rate, one further period was simulated for power input evaluation.

2.6. Cultivation of CHO suspension cells

The utilized CHO suspension cell line XM111-10 (established by Prof. Dr. Martin Fussenegger and team, ETH Zürich, Switzerland [100]; CCOS 837) was cultivated in all investigated cultivation systems. CHO XM111-10 is a model cell line that produces secreted alkaline phosphatase (SEAP) using a tetracycline induced switch-off system (tet-off) [101]. Under non-limiting conditions, the suspension cell culture grown in chemically defined minimal media has a doubling time of approximately 18 h and a peak viable cell density of $4 \cdot 10^6$ cells mL^{-1}, as demonstrated in a traveling wave [102] or stirred tank bioreactor [103]. The cell size distribution of CHO XM111-10 was approximated with a Gaussian normal distribution at an expected value of 14.45 µm and a standard deviation of 1.40 µm (data concerning the cell size distribution can be found in the appendix). This means that with the assumption of a maximum cell size of 20 µm, 99% of the cells can be described. The cells were thawed and transferred into a static cultivation system (75 mL T-flask, Corning Inc., New York, USA) with 20 mL FMX-8 media (Cell Culture Technologies, Gravesano, Switzerland). Subcultivation was done after 48 h and 96 h in T-flasks with cell densities of $0.5 \cdot 10^{-6}$ cells mL^{-1}. After a further 48 h, the cell suspension was transferred into orbitally shaken 1 L flasks (Corning Inc.) for 72 h and finally into the investigated cultivation system, whereby seeding cell densities of $0.5 \pm 0.1 \cdot 10^{-6}$ cells mL^{-1} were used. The ChoMaster HP-1 medium (Cell Culture Technologies), supplemented with 1 mmol L^{-1} L-glutamine (G5792, Sigma-Aldrich), 10mL L^{-1} Pluronic F68 (A1288, AppliChem GmbH, Darmstadt, Germany) and 2.5 mg L^{-1} tetracycline (T7660, Sigma-Aldrich) was used for all orbitally shaken experiments. All cultivations were performed at 37 °C with 7.5% CO_2 saturation and 80% humidity (measured within the shaker unit) at shaking diameters of 25 and 50 mm (Multritron Cell, Infors AG). The filling volume and the shaking rate were varied in an expedient range set by the process engineering characterization, except for the inoculum preparation, which was carried out at 120 rpm, 50 mm and 300 mL filling volume. Cell density (Innovatis Cedex, Roche Diagnostics, Rotkreuz, Switzerland) was measured every 24 h.

2.7. Design space creation and Monte Carlo simulation

To predict the cultivation success, and conversely the probability of failure, a two-dimensional design space was created for each cultivation system and shaking diameter using the filling volume and shaking rate. The response used was the combination of mixing time Θ_M, k_La-value and volumetric power input P/V. This design space corresponds to the concept of ICH [11]. To calculate the probability of failure in the design space, a partitioning into 500 × 500 parts was carried out, followed by a Monte Carlo simulation with 10 000 steps in each case. A normally distributed error was added for each factor with a standard deviation of ± 5% of the factor range [104]. Using a confidence interval of 95% and a standard deviation of 5%, 9 604 iterations are required to obtain a maximum error of 0.1% [105]. In order to undercut the error, 10 000 iterations were chosen. Simulations with at least one value outside the acceptance range were marked as errors, resulting in a probability of error. The boundaries of the individual factors (shaking rate, filling volume) for the design space correspond to the experimental space (see Table 1). The acceptance range was defined by the authors (subsection

3.3) and was a maximum of 20 s for the mixing time, a maximum of 900 W m^{-3} for the volumetric power input and a minimum of 10.5 h^{-1} for the volumetric mass transfer coefficient. The process capability indices and therefore the probabilities of failure were calculated according to Kane [15]. The Monte Carlo simulation was carried out in parallel using the message passing interface on a high-performance computer (Linux CentOS 7.5.1804) with Python 3.6.5 [106].

3. Results and discussion

In this section, the process engineering results are first evaluated and the Kolmogorov approach for orbital shaken cultivation systems is reviewed. Subsequently, the creation of a design space is shown using the 500 mL Erlenmeyer flask as an example before presenting the evaluation of the cultivation systems studied. A detailed review of all cultivation systems is provided in the appendix.

3.1. Process engineering characterization

In Fig. 4, the ranges in values that were found in the process engineering investigations are summarized for all systems. In the investigated space, major differences in the process engineering parameters occurred. In each cultivation system, mixing times below 3 s could be achieved, yet, especially in the 5 L Optimum Growth flask, mixing times could reach several minutes and thus may negatively affect cell growth. At low shaking rates and high filling volumes, all systems were characterized by low k_La values. Nevertheless, using high shaking rates and low filling volumes, both 500 mL flasks produced k_La values over 100 h^{-1} whilst the 600 mL TubeSpin and the 5000 mL Optimum Growth flask reached values above 60 h^{-1}. It should be mentioned that oxygen transfer in the TubeSpin bioreactors could be further increased by using even lower filling volumes or an angled mount inside the shaker [107], but these conditions were not investigated in this study. The volumetric power input varied between 1 W m^{-3} (maximum filling volume, minimum shaking rate, 25 mm shaking diameter) and several kW m^{-3}, whereby by far the highest values could be achieved in the 600 mL TubeSpin (2.3 kW m^{-3}) and the 5000 mL Optimum Growth (3.7 kW m^{-3}). Thus, a wide range of favorable and unfavorable conditions could be found in the five selected cultivation systems.

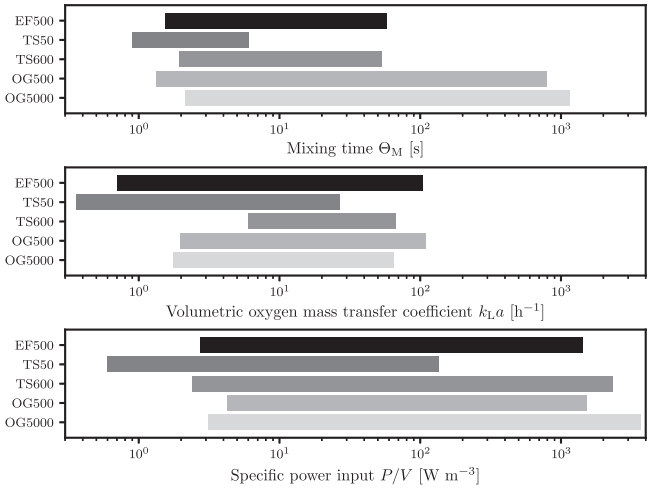

Fig. 4. Overview of the process engineering characterization for all investigated systems. The span of measured values for the mixing time Θ_M (top), volumetric oxygen mass transfer coefficient k_La (middle) and specific power input P/V (bottom) is depicted.

3.2. CHO XM111-10 suspension culture limitations

The inoculum preparation approach described in subsection 2.6 was also used for cell growth limitation studies. Hence, the success of a cultivation should only be affected by process engineering variations. The preliminary experiments were performed in 500 mL Erlenmeyer flasks, as these often serve as a standard cultivation vessel for comparative studies. As can be seen in Fig. 3, the oxygen demand of a CHO cell line varies significantly, depending on the clone and cultivation conditions. Thus, for the investigated CHO XM 111-10 cell line, the specific oxygen demand of $2.8 \cdot 10^{-13}$ mol_{O_2} $cell^{-1}$ h^{-1} was experimentally determined. This can be translated to a minimal k_La using Eq. 1. If, for example, a minimum oxygen concentration of 30% with a maximum expected cell density of $5 \cdot 10^6$ cells mL^{-1} is required, a k_La of 10.5 h^{-1} is needed to ensure oxygen supply. Please note that this k_La-value is slightly higher as it would be in an acid controlled stirred bioreactor (9.7 h^{-1}) due to the 7.5% CO_2 in the incubator atmosphere. The maximum tolerable mixing time was set to 20 s according to Platas Barradas et al. [18]. Determining a critical power input or energy dissipation rate proved to be difficult because (as Chalmers was able to impressively show [87]) limitations or (sub-)lethal effects occur at different values. Therefore, the Kolmogorov microturbulence concept was adopted (Eq. 4) and the maximum energy dissipation rate (Eq. 3) was calculated. The threshold proposed by Peter [95] was used and compared against the created eddy sizes for given volumetric power inputs (Fig. 5). Only with the onset of full turbulent flow and thus an $\varepsilon_{max} > \overline{\varepsilon}$, a vortex size in the order of magnitude of CHO XM111-10 cells was reached. The micro eddies thus reached a critical size in the range of 1 kW m^{-3}, a value that occurred at 275 rpm, 50 mm and 100 mL in 500 mL Erlenmeyer flaks, for example.

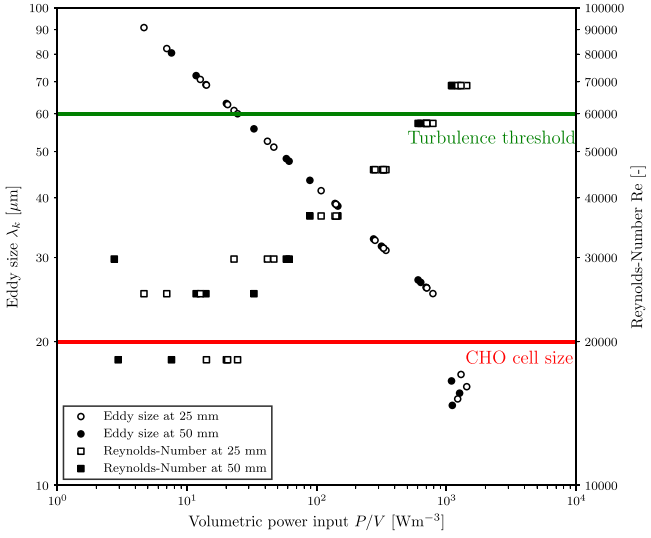

Fig. 5. Calculation of the eddy size (circles) and the Reynolds number (square) inside a 500 mL Erlenmeyer flask against the volumetric power input. Black symbols indicate power input simulations at 25 mm, white at 50 mm shaking diameter. Turbulence threshold was set to $Re = 60\,000$, maximum observed CHO cell size to 20 µm.

3.3. Creating of cell culture design spaces

The limits found in the previous section can now be used to create design spaces. This allows for the verification of all process engineering parameters at the same time. In summary, the following threshold values are used:

- A mixing time Θ_M of 20 s as the upper limit
- A k_La-value of at least 10.5 h^{-1} based on a q_{O_2} of $2.8 \cdot 10^{-13}$ mol_{O_2} $cell^{-1}$ h^{-1} and a maximum cell density of $5 \cdot 10^6$ cells mL^{-1}
- A maximum volumetric power input P/V of 900 Wm^{-3}, leading to eddy sizes above 20 µm

Utilizing these limitations, a design space for every cultivation system was created from which the probability of failure (green to red) with all specifications is visible. As an example, the design space for the 500 mL Erlenmeyer flask is depicted in Fig. 6. Cultivations (presented as white dots) were performed inside and outside the recommended parameter combinations (green area) to evaluate the chosen limitations. If the selected parameter combination cannot be achieved at any point in the system (no green area), a successful cultivation is still possible, but cannot be expected with certainty. Experiments were evaluated primarily by the maximum specific growth rate, which was determined by maximizing the fit of an exponential function. The maximum viable cell density (VCD_{max}) was used as a plausibility check, so that an experiment with $\mu_{max} > 0.04\ h^{-1}$ (doubling time t_d of 17.33 h and $VCD_{max} > 3{\cdot}10^6$ cells mL^{-1} could be considered successful.

3.4. Cultivation results

To verify the design space approach, the 500 mL Erlenmeyer flask was investigated in a first step (with 50 mm shaking diameter, Fig. 7). It was quite clearly demonstrated that experiments within the sweet spot (the green zone in Fig. 7, defined by a probability of failure below 1%) performed as desired ($\mu_{max} > 0.04\ h^{-1}$, $t_d < 17.33$ h), whereas the experiments in the peripheral areas resulted in a reduced maximum specific growth rate ($\mu_{max} < 0.04\ h^{-1}$). The experiments at 110 rpm (outside of the sweet spot but with error probabilities < 50%) also showed the desired maximum specific growth rates, illustrating that exceeding the sweet spot is not immediately associated with a loss of specific growth rate. This can be explained by the still sufficiently high k_La values (> 10 h^{-1}) and low mixing times (< 25 s). However, at 80 rpm and 200 mL filling volume, reduced maximum specific growth rates were measurable ($0.03\ h^{-1} < \mu_{max} < 0.04\ h^{-1}$), which can be explained by the lower k_La value (50% of the target at 200 mL) and mixing times above 30 s. At 300 rpm, in contrast, the cells stopped growing almost completely, which can be explained by the high energy input and the resulting fluid dynamic stress caused by the small eddies. Similar results can be seen using a shaking diameter of 25 mm, where in the case of 80 rpm and 200 mL, sedimentation of the cells could be observed (see appendix). In

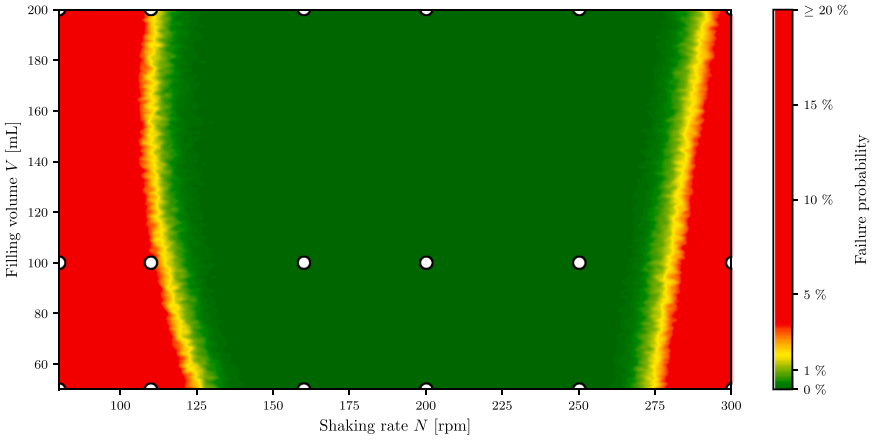

Fig. 6. Design space for the 500 mL Erlenmeyer flask with 50 mm shaking diameter. The probability of failure is colored from green = low to red = high. White circles indicate parameter combinations where cultivations were performed.

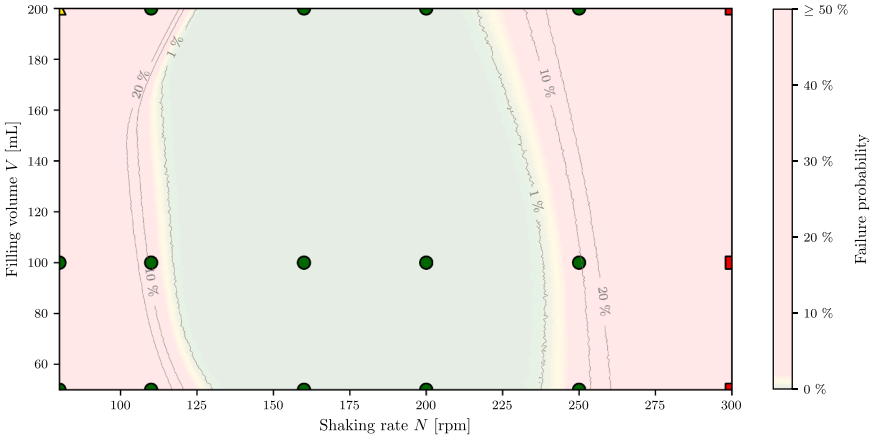

Fig. 7. Evaluation of 500 mL Erlenmeyer flask (50 mm shaking diameter) design space based on the maximum specific growth rate. Green dots indicate experiments that went as desired with a $\mu_{max} > 0.04\ h^{-1}$. Yellow triangles represent underperforming experiments with $0.03\ h^{-1} < \mu_{max} < 0.04\ h^{-1}$, red squares experiments with poor performance $\mu_{max} < 0.03\ h^{-1}$.

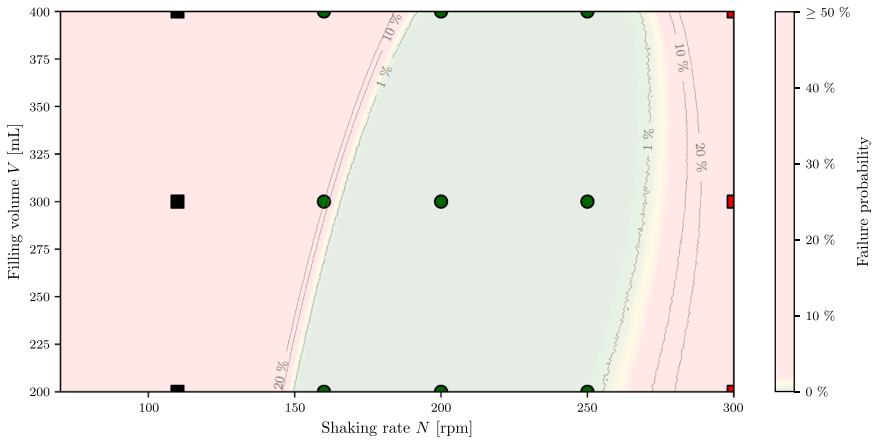

Fig. 8. Evaluation of the 600 mL TubeSpin (25 mm shaking diameter) design space based on the maximum specific growth rate.

summary, the growth of CHO cells in the 500 mL Erlenmeyer flask can be well predicted using the process engineering characterization based design space.

The TubeSpin bioreactors behaved somewhat differently due to their basic cylindrical shape, as the example of the 600 mL TubeSpin at 25 mm shaking diameter demonstrates (Fig. 8). Within the design space (at 160, 200 and 250 rpm), the cultivations proceeded as desired. However, at 110 rpm (corresponding to a mixing time of approximately one minute), the cells sedimented, causing the experiment to fail. Utilizing a shaking rate of 300 rpm and hence power inputs from 0.9 (400 mL) to 1 kW m^{-3} (200 mL), the cells formed macroscopically visible agglomerates and minor growth. Again, the high predictability of the cultivation success was shown by the process engineering limits set in the design space. However, the failure rate in the extreme ranges was much more pronounced compared to the Erlenmeyer flask, which can be explained by the cylindrical shape and the associated significantly increased filling height. Similar effects could be seen for the 50 mL and the 600 mL TubeSpin with 50 mm shaking diameter, whereas sedimentation was more pronounced at 25 mm (see appendix for the design spaces).

The 500 mL Optimum Growth flask showed similar behavior to the 500 mL Erlenmeyer flask, although the higher maximum filling volume may have a negative effect on cultivation success at low shaking rates and high filling volumes (e.g. at 90 rpm, 250 mL and 25 mm shaking diameter), which can be justified by poorer mixing. This effect is even more visible with the 5 L Optimum Growth flask, so it is recommended to avoid combining a high filling volume with a lower shaking rate when using these flasks. At the same time, the larger inner diameter leads to high power inputs at shaking rates $>$ 200 rpm, through which the sweet spot in this cultivation system is significantly smaller (the corresponding design spaces can be found in the appendix.) Interestingly, the 5 L flask with a 3 L filling volume could not achieve the desired maximum specific growth rates and cell densities within the sweet spot, revealing a weakness in the design space concept. At the maximum filling volume and shaking rates $>$ 110 rpm, a foam layer several centimeters high formed, which limited the oxygen transfer and was not evident from the process engineering investigations. Comparing the maximum specific growth rates of all experiments, it can be seen that the median for all is between 0.033 and 0.042 h^{-1}. The 500 mL Erlenmeyer and Optimum Growth flask are characterized by the highest median specific growth rates (0.041 and 0.043 h^{-1}, respectively) with a smaller interquartile range, which demonstrates the relative independence of the selected process engineering parameter combinations. Both TubeSpin bioreactors are distinguished by more outliers and failed experiments due to cell sedimentation, reflecting a more limited set of parameters.

4. Conclusion

The application of characterization-based process engineering, multi parameter design spaces is a promising way to improve cultivation success in orbitally shaken cultivation systems. This was demonstrated with the investigation of differently shaped cultivation systems (Erlenmeyer flask, TubeSpin bioreactor and Optimum Growth flask) utilizing CHO XM111-10 cells. Within the sweet spot (the region in the design space with an error probability below 1%), the experiments showed targeted maximum specific growth rates ($\mu_{max} > 0.04$ h^{-1}) and cell densities ($VCD_{max} > 3{\cdot}10^6$ cells mL^{-1}). In its immediate vicinity, both ideal and slightly reduced maximum specific growth rates were observed, whereas cultivations in the peripheral areas often led to failures due to lack of mixing, sedimentation, reduced oxygen availability or high fluid dynamic stress. Extreme conditions atypical for mammalian cell cultures (for example, volumetric power inputs exceeding 1 kW m^{-3}) were selected to demonstrate the applicability of the Kolmogorov eddy size concept for predicting stress-induced limitations in shake flasks. As predicted, growth reduction occurred once the minimum vortex size equaled the cell size. This may be less of a limiting factor for CHO suspension cells in shake flasks, but may be critical when applying the approach of this case study to highly aggregating (e.g. HEK 293) or larger cells (e.g. plants suspension cultures) or microcarrier-dependent cell lines (e.g. stem cells).

For the user, this means that combinations of shaking rate, filling volume and shaking diameter which ensure results within the sweet spot can be used for this investigated cell line to achieve comparable results with targeted growth rates and cell densities. For implementation, the process engineering data of the cultivation systems as well as potentially critical factors of the cell lines must be known or determined. It should be noted that in this study, broad design spaces were deliberately selected, which require an increased number of process engineering experiments. This has the advantage that no further characterization is necessary when transferring to other cell lines. However, the process engineering experimental effort can be significantly reduced by appropriately preselecting parameters.

After the initial characterization step, the approach can be used in different ways: First, cultivation success can be ensured in orbitally shaken systems (for instance for inoculum production), even if factors such as vessel size, shaking rate or filling volume change. Furthermore, the approach – by adapting the cell line-specific limitations (cell size and associated sensitivity to fluid dynamic stress, cell-specific oxygen demand, and metabolic influences due to insufficient mixing) – can be used for other cell lines with little effort. The data required for this purpose can be obtained from suitable literature or experiments and compared with the already known characteristics of the cultivation systems, although proof-of-concept cultivations are recommended. Finally, the chosen approach can also be used for non-shaken cultivation systems, since the mixing time, k_La value or power input can be determined for stirred or well-mixed bioreactors as well. This allows for better comparability between differently powered cultivation systems as well as a simplified scale-up, since the used and confirmed cell specific limits for oxygen supply, mixing time and mechanical damage can be transferred. The chosen approach thus allows for cultivations with the desired growth in different orbital shaken cultivation systems, a characterization of the selected cell line and hence knowledge for the transfer to larger systems, just with simple means and without additional sensors – based on procedural characterization alone.

CRediT authorship contribution statement

Rüdiger W. Maschke: Conceptualization, Investigation, Writing - Original Draft, Visualization, Preparation of manuscript revision. **Stefan Seidel**: Software, Formal analysis, Data curation, Visualization, Writing - Review & Editing, Review of manuscript revision. **Thomas Bley**: Writing - Review & Editing. **Regine Eibl**: Writing - Review & Editing **Dieter Eibl**: Project administration, Funding acquisition, Writing - Review & Editing.

Declaration of Competing Interest

The authors declare that they have no known competing financial interests or personal relationships that could have appeared to influence the work reported in this paper.

Acknowledgments

This work was funded by the Swiss Innovation Agency - Innosuisse (https://www.innosuisse.ch/inno/en/home.html) within the project CTI 16924.1 PFLS-LS. The authors would like to thank Jolanda Meister, Philipp Hecht, and Nils Wagner for experimental work and Jason Roger Parry for language editing.

Appendix

The approach outlined in this publication is applied in this digital appendix to all systems as a case study to ensure replicability and to enable application to other cell lines. The process characterization (Θ_M, k_La, P/V) is performed as described in chapter 2. Based on this, mathematical derivations are created, which can be used for the selected system for all potential cell lines. For CHO XM111-10 (the selected cell line for this case study), we defined the following critical parameters:

- A mixing time Θ_M of 20 s
- A q_{O_2} of $2.8 \cdot 10^{-13}$ mol_{O_2} $cell^{-1}$ h^{-1}
- A maximum cell size of 20 µm
- A maximum cell density of $5 \cdot 10^6$cells mL^{-1}

Knowing the limitations of the cell line, the process engineering parameters can be set accordingly to create the design spaces with the following desirable conditions:

- A mixing time Θ_M below 20 s
- A k_La-value above 10.5 h^{-1}
- A volumetric power input P/V below 900 W m^{-3}, leading to eddy sizes above 20 µm

With these settings, the design spaces were created (adapted to the engineering parameters of every system and the requirements for the CHO XM111-10 cell line) and cultivations were conducted. The following evaluation was applied:

- Successful cultivations with a $\mu_{max} > 0.04$ h^{-1} and a $VCD_{max} > 3 \cdot 10^6$cells mL^{-1} are indicated with green dots.
- Acceptable cultivations with 0.03 $h^{-1} < \mu_{max} < 0.04$ h^{-1} and a $VCD_{max} > 2.5 \cdot 10^6$cells mL^{-1} are marked as yellow triangles.
- Cultivations with poor performance $\mu_{max} < 0.03$ h^{-1} are indicated with red squares.
- Black squares indicate experiments without growth, e.g. due to cell sedimentation.

500 mL Erlenmeyer flask

The design space of the 500 mL Erlenmeyer flask proved to be robust (Fig. 9). In the range of 80–250 rpm, successful cultivations can be expected at both shaking diameter regardless of the filling volume. The only exception is the combination of the minimum shaking rate (80 rpm) with the maximum filling volume (200 mL), which leads to sedimentation at 25 mm shaking diameter and reduced growth at 50 mm. At the maximum shaking rate (300 rpm), the critical vortex size of 20 µm is undercut, resulting in slow growth with maximum cell densities of $1 \cdot 10^6$ cells mL^{-1} and a 3–4 d lag phase.

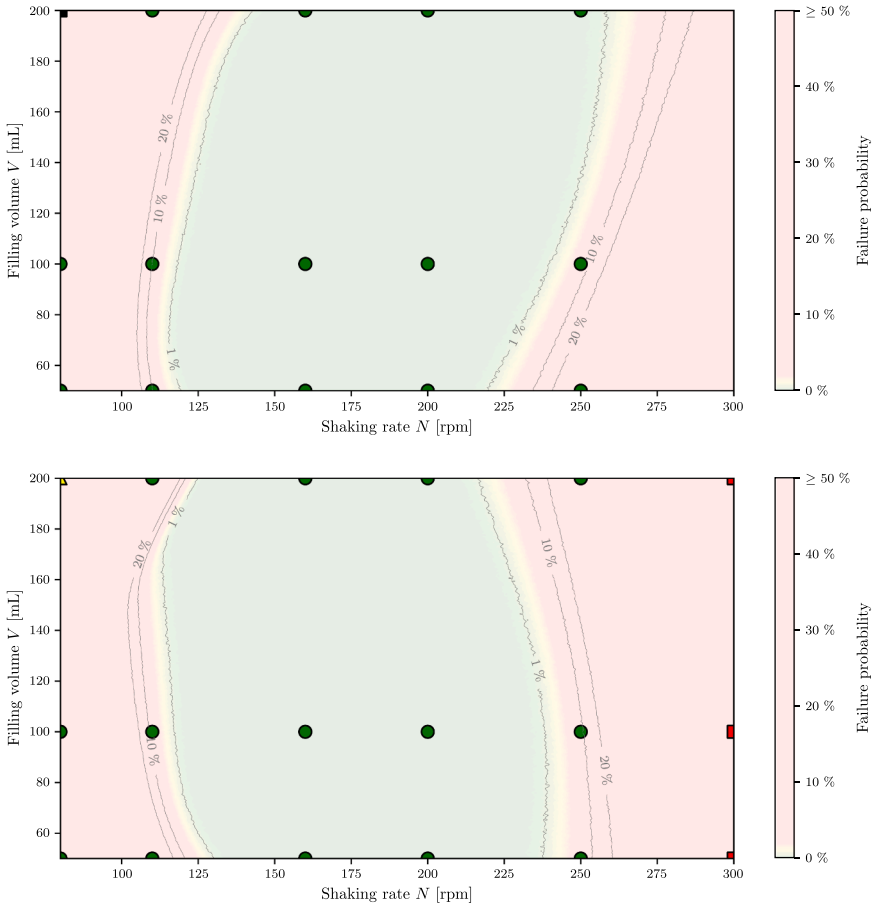

Fig. 9. Evaluation of the 500 mL Erlenmeyer flask design spaces with 25 mm (top) or 50 mm (bottom) shaking diameter based on the maximum specific growth rate.

500 mL Optimum Growth flask

Compared to the 500 mL Erlenmeyer flask, the sweet spot for the 500 mL Optimum Growth flask at 25 mm shaking diameter is smaller (Fig. 10). Especially at high filling volumes (250 mL) with low shaking rates, the cells may grow poorly (VCD_{max} of $1.67 \cdot 10^6$ cells mL^{-1} and μ_{max} of 0.02 h^{-1} at 90 rpm) or with a reduced maximum specific growth rate (μ_{max} of 0.038 h^{-1} at 150 rpm). Due to the higher k_La values and the lower mixing times, the growth at 50 mm shaking diameter is still good at low shaking rates and high filling volumes, so the use of the 500 mL Optimum Growth flask with 50 mm shaking diameter is recommended. At shaking rates of 250 rpm and filling volumes of 50 mL (corresponding to power input values of approx. 0.7 kW m^{-3}), a reduced maximum specific growth rate (μ_{max} of 0.036 h^{-1}) was observed independent of the shaking diameter, thus setting the upper limit.

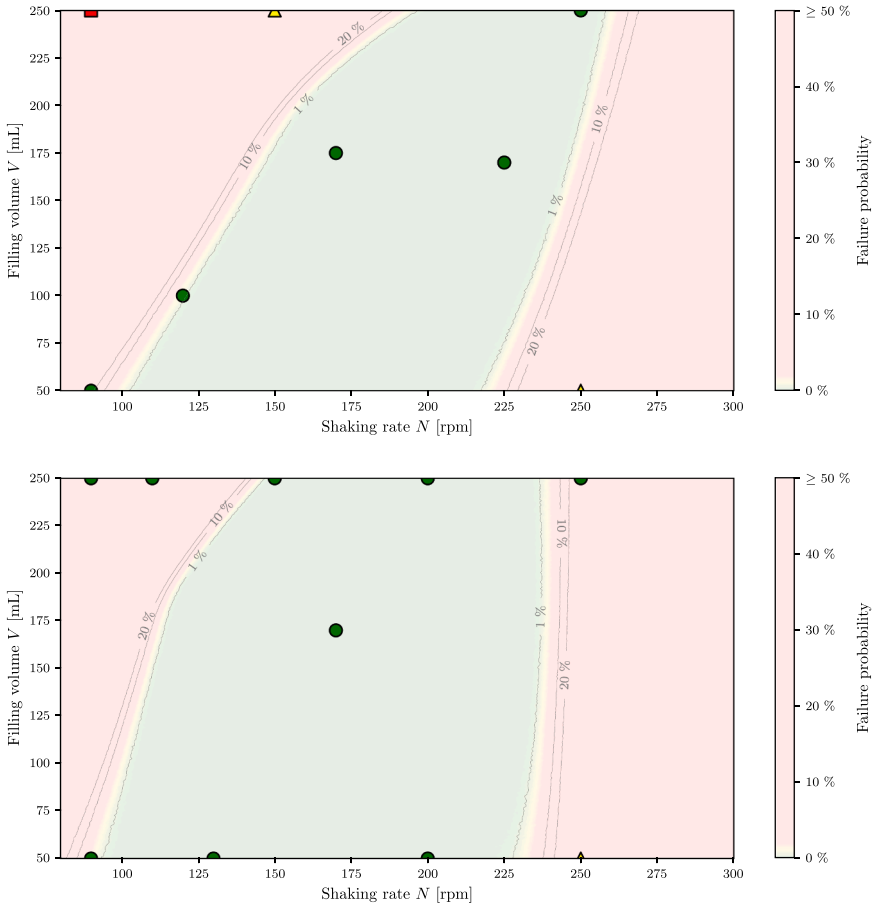

Fig. 10. Evaluation of the 500 mL Optimum growth flask design spaces with 25 mm (top) or 50 mm (bottom) shaking diameter based on the maximum specific growth rate.

5000 mL Optimum Growth flask

The 5000 mL Optimum Growth flask has the narrowest sweet spot of all investigated cultivation systems (Fig. 11). This can be explained by the high volumetric power input (e.g. above 1 kW m^{-3} at 180 rpm and filling volumes of 1200 mL) for the upper limit as well as the high mixing times at low shaking rates and high filling volumes (e.g. above 7 min at 90 rpm and filling volumes of 3000 mL with 25 mm shaking diameter). Furthermore, increased foaming was observed for parameter combinations with high filling volumes and high shaking rates (e.g. 200 and 250 rpm with 3000 mL using a shaking diameter of 25 mm or 150 and 170 rpm with 3000 mL using a shaking diameter of 50 mm). This seems to be a limitation of the design space approach, as foam formation could not be predicted by the process engineering characterization.

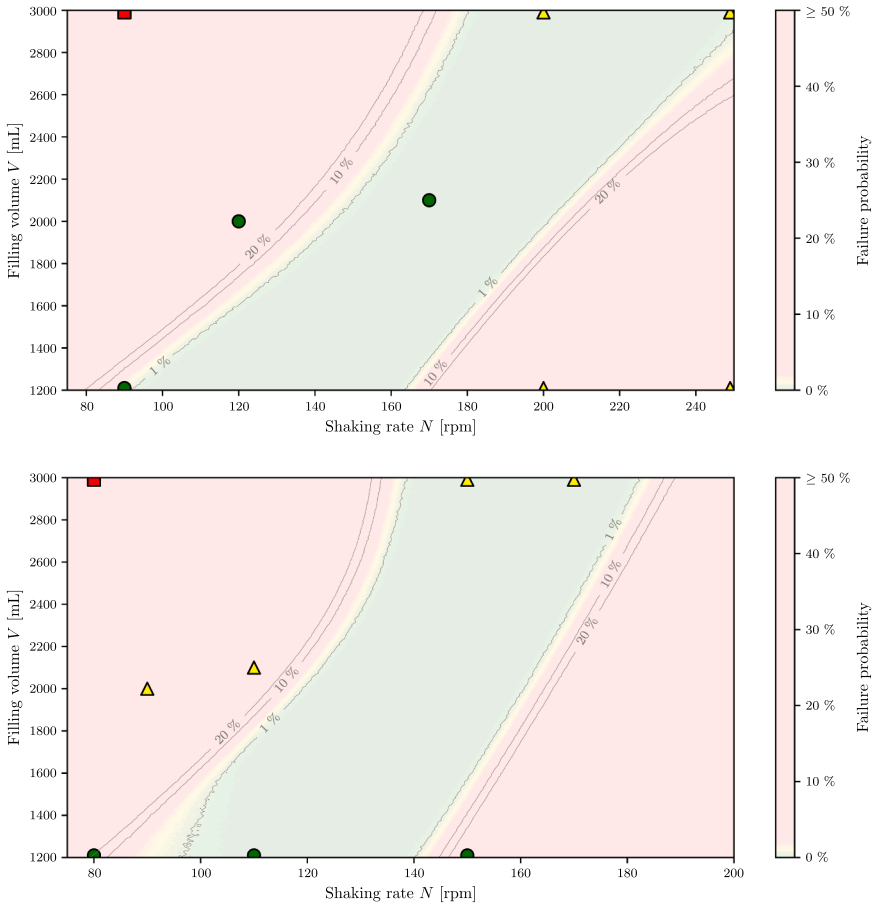

Fig. 11. Evaluation of the 5000 mL Optimum growth flask design spaces with 25 mm (top) or 50 mm (bottom) shaking diameter space based on the maximum specific growth rate.

50 mL TubeSpin

The sweet spot for the 50 mL TubeSpin bioreactor is primarily within the range of high shake rates (> 160 rpm at 25 mm and > 110 rpm at 50 mm shaking diameter, Fig. 12). The lower boundaries are marked by cell sedimentation, which is even more pronounced in this cylindrical vessels at higher filling volumes (see results of 10 and 30 mL at the boarder of the sweet spots). At the maximum shaking rate (300 rpm), the formation of macroscopic aggregates was observed, which was accompanied by a reduction in the maximum specific growth rate.

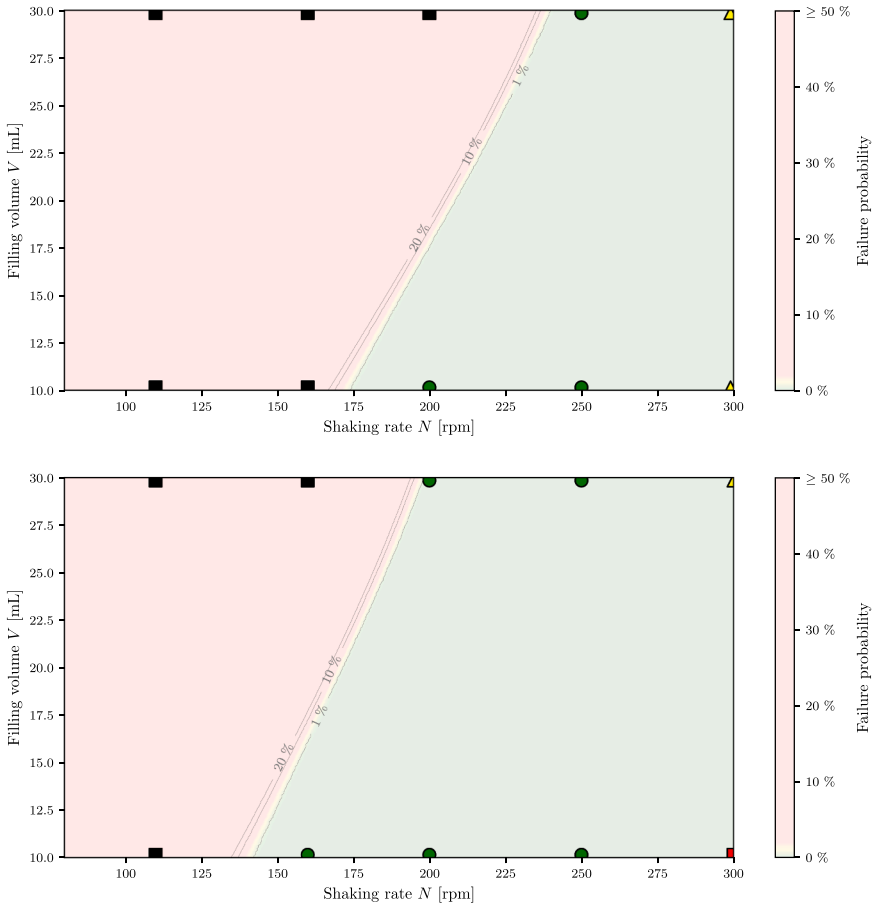

Fig. 12. Evaluation of the 50 mL TubeSpin design spaces with 25 mm (top) or 50 mm (bottom) shaking diameter based on the maximum specific growth rate.

600 mL TubeSpin

The 600 mL TubeSpin bioreactor has a design space comparable to the 500 mL Erlenmeyer and Optimum Growth flask (Fig. 13). However, cultivations outside the sweet spot lead to unfavorable conditions more quickly. Shaking rates below 110 rpm at 25 mm shaking diameter led to cell sedimentation. Utilizing the maximum shaking rate of 300 rpm caused a reduced maximum specific growth rate ($\mu_{max} < 0.030$ h^{-1} at 25 mm and $\mu_{max} < 0.023$ h^{-1} at 3.0 mm shaking diameter with $VCD_{max} < 2{\cdot}10^6$ cells mL^{-1} and $VCD_{max} < 1.6{\cdot}10^6$ cells mL^{-1} respectively). The transition from optimal to fluid mechanically damaging conditions is observable at 250 rpm at 50 mm shaking diameter, where the maximum specific growth rate is reduced to 0.032 h^{-1} with VCD_{max} of $2.5 \cdot 10^6$ cells mL^{-1}.

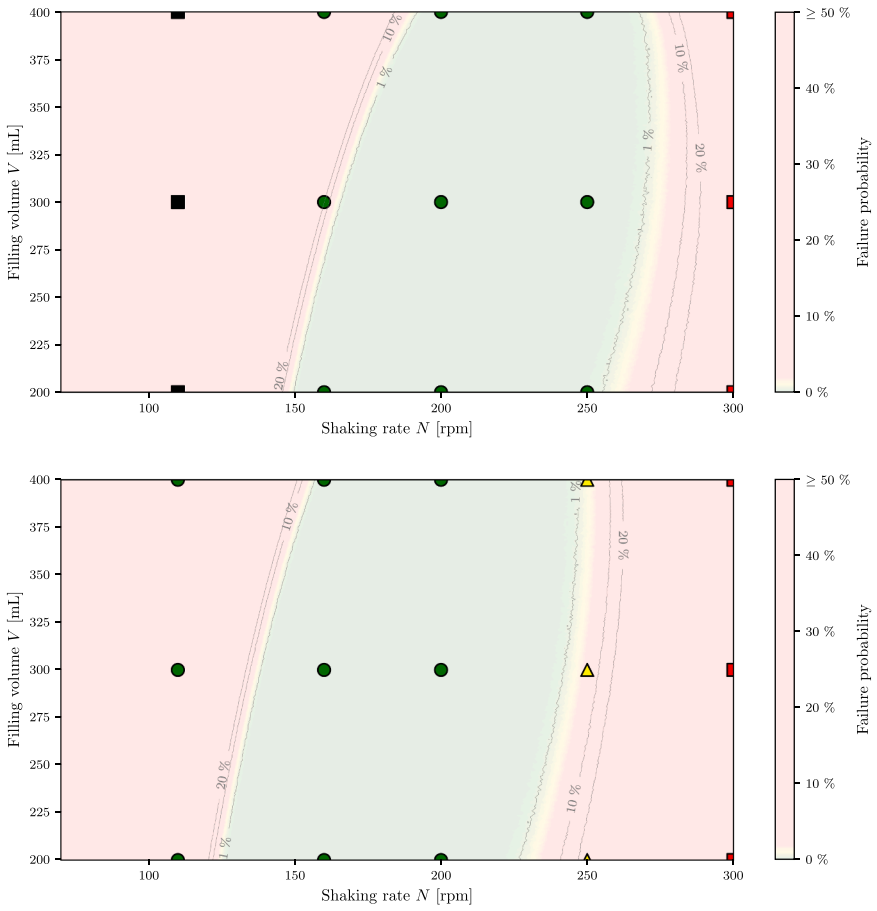

Fig. 13. Evaluation of the 600 mL TubeSpin design spaces with 25 mm (top) or 50 mm (bottom) shaking diameter based on the maximum specific growth rate.

Cell size distribution

To assess the effect of eddy-generated shear stress on the cells, the cell size distribution had to be determined at different time points. The measurements were made with a Cedex HiRes, by which the class width of 1 µm was fixed. The data was subsequently applied to a Gaussian normal distribution function in order to make simpler numerical statements about the cell size distribution over the course of cultivation (Fig. 14). On average, the expected value μ of cell size was 14.45 µm with a standard deviation σ of 1.40 µm, which means that 99% of the cells can be assumed to be smaller than 20 µm, the selected upper cell size limit in this study.

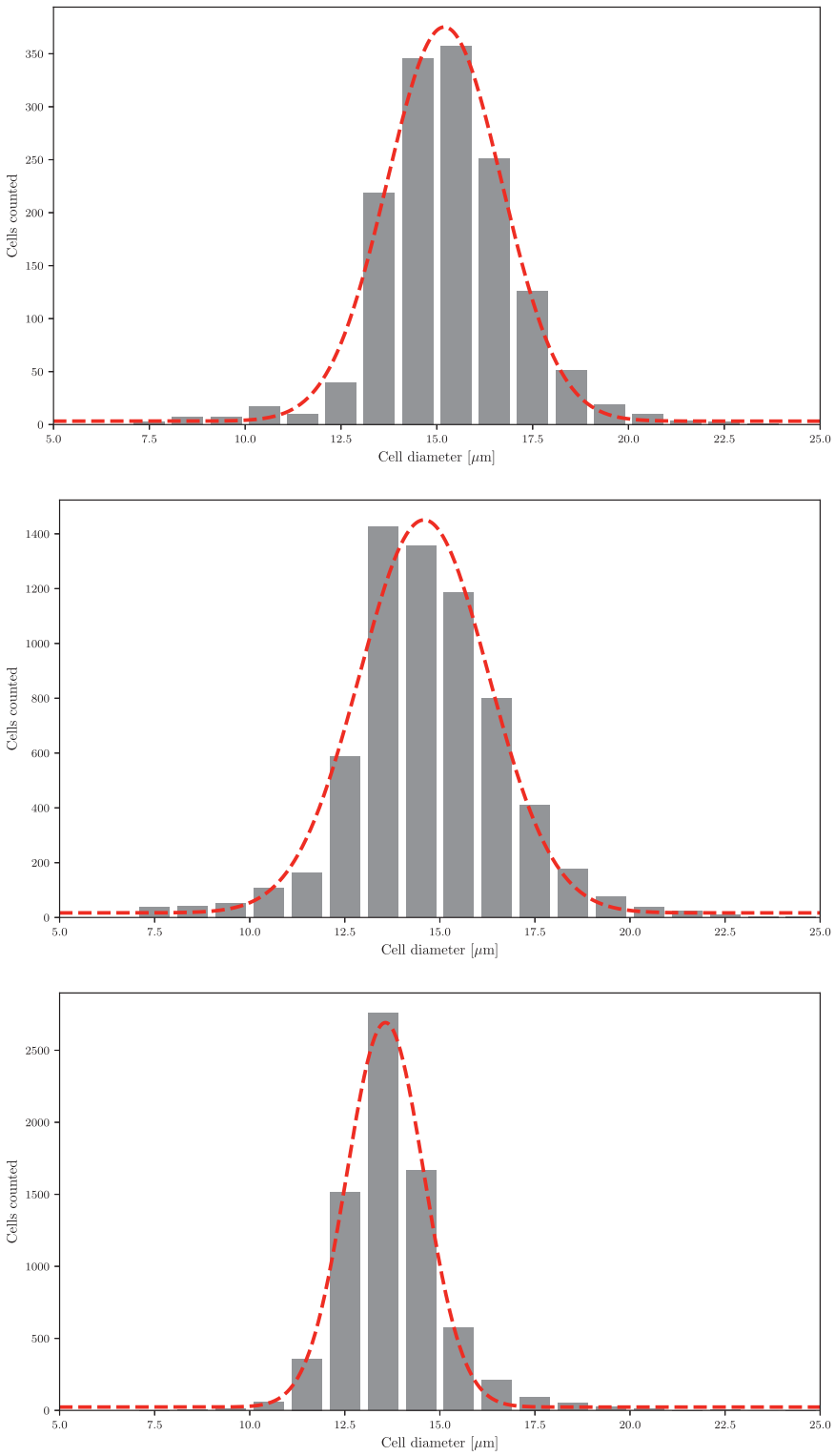

Fig. 14. Cell size distribution and Gaussian fit of CHO XM111-10 cells cultivated in a 500 mL Erlenmeyer flask at the beginning of the exponential growth phase (top, $\mu = 15.20$ µm, $\sigma = 1.50$ µm), the end of the exponential growth phase (middle, $\mu = 14.59$ µm, $\sigma = 1.70$ µm) and in the stationary phase (bottom, $\mu = 13.57$ µm, $\sigma = 1.02$ µm).

References

[1] E.S. Langer, D.E. Gillespie, R. Rader (Eds.), 17th Annual Report and Survey on Biopharmaceutical Manufacturing Capacity and Production, 17th edition, BioPlan Associates, Inc., Rockville, MD, 2020.

[2] O. Krätz, Das Portrait: Emil Erlenmeyer 1825-1909, Chem. Unserer Zeit 6 (2) (1972) 53–58, https://doi.org/10.1002/ciuz.19720060204.

[3] W. Klöckner, J. Büchs, Advances in shaking technologies, Trends Biotechnol. 30 (6) (2012) 307–314, https://doi.org/10.1016/J.TIBTECH.2012.03.001.

[4] K. Winkler, M.L. Socher, Shake Flask Technology, in: Encyclopedia of Industrial Biotechnology, John Wiley & Sons, Inc., Hoboken, NJ, USA, 2014, pp. 1–16, https://doi.org/10.1002/9780470054581.eib651.

[5] M. Torres, M. Elvin, Z. Betts, S. Place, C. Gaffney, A.J. Dickson, Metabolic profiling of Chinese hamster ovary cell cultures at different working volumes and

agitation speeds using spin tube reactors, Biotechnol. Prog. (2020), e3099, https://doi.org/10.1002/btpr.3099.
[6] D.L. Hacker, L. Durrer, S. Quinche, CHO and HEK293 Cultivation and Transfection in Single-Use Orbitally Shaken Bioreactors, in: Methods in Molecular Biology, Springer, New York, 2018, pp. 123–131, https://doi.org/10.1007/978-1-4939-8730-6_9.
[7] N. Gomez, M. Ambhaikar, L. Zhang, C.-J. Huang, H. Barkhordarian, J. Lull, C. Gutierrez, Analysis of Tubespins as a suitable scale-down model of bioreactors for high cell density CHO cell culture, Biotechnol. Prog. 33 (2) (2017) 490–499, https://doi.org/10.1002/btpr.2418.
[8] J. Meister, R.W. Maschke, S. Werner, G.T. John, D. Eibl, How to efficiently shake viscous vulture broths, Genet. Eng. Biotechnol. N. 36 (15) (2016) 28–29, https://doi.org/10.1089/gen.36.15.14.
[9] J. Scholz, S. Suppmann, A re-usable wave bioreactor for protein production in insect cells, MethodsX 3 (2016) 497–501, https://doi.org/10.1016/j.mex.2016.08.001.
[10] S. Seidel D. Eibl Influence of Interfacial Force Models and Population Balance Models on the kLa Value in Stirred Bioreactors Processes 9 7 10.3390/pr9071185.
[11] International Conference on Harmonisation of Technical Requirements for Registration of Pharmaceuticals for Human Use, Pharmaceutical Development Q8 (R2) (2009).
[12] A.S. Rathore, Roadmap for implementation of quality by design (QbD) for biotechnology products, Trends Biotechnol. 27 (9) (2009) 546–553, https://doi.org/10.1016/j.tibtech.2009.06.006.
[13] H.B. Grangeia, C. Silva, S.P. Simões, M.S. Reis, Quality by design in pharmaceutical manufacturing: a systematic review of current status, challenges and future perspectives, Eur. J. Pharm. Biopharm. 147 (2020) 19–37, https://doi.org/10.1016/j.ejpb.2019.12.007.
[14] S.F. Abu-Absi, L.Y. Yang, P. Thompson, C. Jiang, S. Kandula, B. Schilling, A. A. Shukla, Defining process design space for monoclonal antibody cell culture, Biotechnol. Bioeng. 106 (6) (2010) 894–905, https://doi.org/10.1002/bit.22764.
[15] V.E. Kane, Process Capability Indices, J. Qual. Technol. 18 (1) (1986) 41–52, https://doi.org/10.1080/00224065.1986.11978984.
[16] X. Gong, Y. Li, H. Chen, H. Qu, Design space development for the extraction process of Danhong injection using a Monte Carlo simulation method, PLoS ONE 10 (5) (2015) 1–20, https://doi.org/10.1371/journal.pone.0128236.
[17] J.J. Peterson, A Bayesian approach to the ICH Q8 definition of design space, J. Biopharm. Stat. 18 (5) (2008) 959–975, https://doi.org/10.1080/10543400802278197.
[18] O. Platas Barradas, U. Jandt, L.D. MinhPhan, M.E. Villanueva, M. Schaletzky, A. Rath, S. Freund, U. Reichl, E. Skerhutt, S. Scholz, T. Noll, V. Sandig, R. Pörtner, A.P. Zeng, Evaluation of criteria for bioreactor comparison and operation standardization for mammalian cell culture, Eng. Life Sci. 12 (5) (2012) 518–528, https://doi.org/10.1002/elsc.201100163.
[19] S. Pereira, H.F. Kildegaard, M.R. Andersen, Impact of CHO metabolism on cell growth and protein production: an overview of toxic and inhibiting metabolites and nutrients, Biotechnol. J. 13 (3) (2018), 1700499, https://doi.org/10.1002/biot.201700499.
[20] S.L.C. Ferreira, R.E. Bruns, E.G.P. daSilva, W.N.L. dosSantos, C.M. Quintella, J. M. David, J.B. de Andrade, M.C. Breitkreitz, I.C.S.F. Jardim, B.B. Neto, Statistical designs and response surface techniques for the optimization of chromatographic systems (data Analysis in Chromatography), J. Chromatogr. A 1158 (1) (2007) 2–14, https://doi.org/10.1016/j.chroma.2007.03.051.
[21] S. Bhattacharya, Central composite design for response surface methodology and its application in pharmacy. Response Surface Methodology in Engineering Science [Working Title], IntechOpen, 2021, https://doi.org/10.5772/intechopen.95835.
[22] C. Löffelholz, S.C. Kaiser, M. Kraume, R. Eibl, D. Eibl. Dynamic Single-Use Bioreactors Used in Modern Liter- and m3- Scale Biotechnological Processes: Engineering Characteristics and Scaling Up, Springer Berlin Heidelberg,, Berlin, Heidelberg, 2014, pp. 1–44, https://doi.org/10.1007/10_2013_187.
[23] C. Löffelholz. CFD als Instrument zur bioverfahrenstechnischen Charakterisierung von single-use Bioreaktoren und zum Scale-up für Prozesse zur Etablierung und Produktion von Biotherapeutika, Phd, Brandenburgischen Technischen Universität Cottbus, 2013.
[24] E. Anane, I.M. Knudsen, G.C. Wilson, Scale-down cultivation in mammalian cell bioreactors–the effect of bioreactor mixing time on the response of CHO cells to dissolved oxygen gradients, Biochem. Eng. J. 166 (2021), 107870, https://doi.org/10.1016/j.bej.2020.107870.
[25] S. Xu, R. Jiang, R. Mueller, N. Hoesli, T. Kretz, J. Bowers, H. Chen, Probing lactate metabolism variations in large-scale bioreactors, Biotechnol. Prog. 34 (3) (2018) 756–766, https://doi.org/10.1002/btpr.2620.
[26] K. Paul, T. Hartmann, C. Posch, D. Behrens, C. Herwig, Investigation of cell line specific responses to pH inhomogeneity and consequences for process design, Eng. Life Sci. 20 (9–10) (2020) 412–421, https://doi.org/10.1002/elsc.202000034.
[27] R.K. Tan, W. Eberhard, J. Büchs, Measurement and characterization of mixing time in shake flasks, Chem. Eng. Sci. 66 (3) (2011) 440–447, https://doi.org/10.1016/j.ces.2010.11.001.
[28] G. Rodriguez, T. Anderlei, M. Micheletti, M. Yianneskis, A. Ducci, On the measurement and scaling of mixing time in orbitally shaken bioreactors, Biochem. Eng. J. 82 (2014) 10–21, https://doi.org/10.1016/j.bej.2013.10.021.
[29] G. Rodriguez, M. Micheletti, A. Ducci, Macro- and micro-scale mixing in a shaken bioreactor for fluids of high viscosity, Chem. Eng. Res. Des. 132 (2018) 890–901, https://doi.org/10.1016/j.cherd.2018.01.018.
[30] D.T. Monteil, G. Tontodonati, S. Ghimire, L. Baldi, D.L. Hacker, C.A. Bürki, F. M. Wurm, Disposable 600-mL orbitally shaken bioreactor for mammalian cell cultivation in suspension, Biochem. Eng. J. 76 (2013) 6–12, https://doi.org/10.1016/j.bej.2013.04.008.
[31] M. Kraume, Mixing times in stirred suspensions, Chem. Eng. Technol. 15 (1992) 313–318, https://doi.org/10.1002/ceat.270150505.
[32] T. Menisher, M. Metghalchi, E.B. Gutoff, Mixing studies in bioreactors, Bioprocess Eng. 22 (2000) 115–120, https://doi.org/10.1007/s004490050020.
[33] Bauer I., Dreher T., Eibl D., Glöckler R., Husemann U., John G.T., Kaiser S.C., Kampeis P., Kauling J., Kleebank S., Kraume M., Kuhlmann W., Löffelholz C., Meusel W., Möller J., Pörtner R., Sieblist C., Tscheschke B., Werner S., Recommendations for process engineering characterisation of single-use bioreactors and mixing systems by using experimental methods (2nd Edition), Tech. rep., Frankfurt am Main (Dec. 2020).
[34] B.A. Wagner, S. Venkataraman, G.R. Buettner, The rate of oxygen utilization by cells, Free Radic. Biol. Med. 51 (3) (2011) 700–712, https://doi.org/10.1016/j.freeradbiomed.2011.05.024.
[35] F. Garcia-Ochoa, E. Gomez, V.E. Santos, J.C. Merchuk, Oxygen uptake rate in microbial processes: an overview, Biochem. Eng. J. 49 (3) (2010) 289–307, https://doi.org/10.1016/j.bej.2010.01.011.
[36] S. Seidel, R.W. Maschke, S. Werner, V. Jossen, D. Eibl, Oxygen mass transfer in biopharmaceutical processes: numerical and experimental approaches, Chem. Ing. Tech. 93 (1–2) (2021) 42–61, https://doi.org/10.1002/cite.202000179.
[37] G. Lovrecz, P. Gray, Use of on-line gas analysis to monitor recombinant mammalian cell cultures, Cytotechnology 14 (3) (1994) 167–175, https://doi.org/10.1007/BF00749613.
[38] P. Jorjani, S.S. Ozturk, Effects of cell density and temperature on oxygen consumption rate for different mammalian cell lines, Biotechnol. Bioeng. 64 (3) (1999) 349–356, https://doi.org/10.1002/(SICI)1097-0290(19990805)64:3<349::AID-BIT11>3.0.CO;2-V.
[39] R.D. Guarino, L.E. Dike, T.A. Haq, J.A. Rowley, J.B. Pitner, M.R. Timmins, Method for determining oxygen consumption rates of static cultures from microplate measurements of pericellular dissolved oxygen concentration, Biotechnol. Bioeng. 86 (7) (2004) 775–787, https://doi.org/10.1002/bit.20072.
[40] C.S. Lai, L.E. Hopwood, J.S. Hyde, S. Lukiewicz, ESR studies of O2 uptake by Chinese hamster ovary cells during the cell cycle, Proc. Natl. Acad. Sci. U. S. A. 79 (6280170) (1982) 1166–1170, https://doi.org/10.1073/pnas.79.4.1166.
[41] C.T. Goudar, J.M. Piret, K.B. Konstantinov, Estimating cell specific oxygen uptake and carbon dioxide production rates for mammalian cells in perfusion culture, Biotechnol. Prog. 27 (5) (2011) 1347–1357, https://doi.org/10.1002/btpr.646.
[42] Z. Xing, B.M. Kenty, Z.J. Li, S.S. Lee, Scale-up analysis for a CHO cell culture process in large-scale bioreactors, Biotechnol. Bioeng. 103 (4) (2009) 733–746, https://doi.org/10.1002/bit.22287.
[43] P.E. James, S.K. Jackson, O.Y. Grinberg, H.M. Swartz, The effects of endotoxin on oxygen consumption of various cell types in vitro: an EPR oximetry study, Free Radic. Biol. Med. 18 (4) (1995) 641–647, https://doi.org/10.1016/0891-5849(94)00179-N.
[44] P. Ducommun, P.A. Ruffieux, M.P. Furter, I. Marison, U. vonStockar, A new method for on-line measurement of the volumetric oxygen uptake rate in membrane aerated animal cell cultures, J. Biotechnol. 78 (2) (2000) 139–147, https://doi.org/10.1016/S0168-1656(99)00237-0.
[45] P. Ducommun, P.A. Ruffieux, A. Kadouri, U. VonStockar, I.W. Marison, Monitoring of temperature effects on animal cell metabolism in a packed bed process, Biotechnol. Bioeng. 77 (7) (2002) 838–842, https://doi.org/10.1002/bit.10185.
[46] K. Xie, X.-W. Zhang, L. Huang, Y.-T. Wang, Y. Lei, J. Rong, C.-W. Qian, Q.-L. Xie, Y.-F. Wang, A. Hong, S. Xiong, On-line monitoring of oxygen in Tubespin, a novel, small-scale disposable bioreactor, Cytotechnology 63 (2011) 345–350, https://doi.org/10.1007/s10616-011-9361-x.
[47] D.R. Gray, S. Chen, W. Howarth, D. Inlow, B.L. Maiorella, CO_2 in large-scale and high-density CHO cell perfusion culture, Cytotechnology 22 (1) (1996) 65–78, https://doi.org/10.1007/BF00353925.
[48] A. Super, N. Jaccard, M.P.C. Marques, R.J. Macown, L.D. Griffin, F.S. Veraitch, N. Szita, Real-time monitoring of specific oxygen uptake rates of embryonic stem cells in a microfluidic cell culture device, Biotechnol. J. 11 (9) (2016) 1179–1189, https://doi.org/10.1002/biot.201500479.
[49] J. Berrios, C. Altamirano, N. Osses, R. Gonzalez, Continuous CHO cell cultures with improved recombinant protein productivity by using mannose as carbon source: Metabolic analysis and scale-up simulation, Chem. Eng. Sci. 66 (11) (2011) 2431–2439, https://doi.org/10.1016/j.ces.2011.03.011.
[50] R. Heidemann, D. Lütkemeyer, H. Büntemeyer, J. Lehmann, Effects of dissolved oxygen levels and the role of extra- and intracellular amino acid concentrations upon the metabolism of mammalian cell lines during batch and continuous cultures, Cytotechnology 26 (3) (1998) 185–197, https://doi.org/10.1023/A:1007917409455.
[51] R.P. Nolan, K. Lee, Dynamic model of CHO cell metabolism, Metab. Eng. 13 (1) (2011) 108–124, https://doi.org/10.1016/j.ymben.2010.09.003.
[52] M. Pappenreiter, B. Sissolak, W. Sommeregger, G. Striedner, Oxygen uptake rate soft-sensing via dynamic kLa computation: cell volume and metabolic transition prediction in mammalian bioprocesses, Front. Bioeng. Biotechnol. 7 (2019) 195, https://doi.org/10.3389/fbioe.2019.00195.
[53] R.R. Deshpande, E. Heinzle, On-line oxygen uptake rate and culture viability measurement of animal cell culture using microplates with integrated oxygen sensors, Biotechnol. Lett. 26 (9) (2004) 763–767, https://doi.org/10.1023/B:BILE.0000024101.57683.6d.

[54] R.R. Deshpande, E. Heinzle, Online monitoring of oxygen in spinner flasks, Biotechnol. Lett. 31 (5) (2009) 665–669, https://doi.org/10.1007/s10529-009-9919-2.

[55] Y.-M. Huang, W. Hu, E. Rustandi, K. Chang, H. Yusuf-Makagiansar, T. Ryll, Maximizing productivity of CHO cell-based fed-batch culture using chemically defined media conditions and typical manufacturing equipment, Biotechnol. Prog. 26 (5) (2010) 1400–1410, https://doi.org/10.1002/btpr.436.

[56] Y. Rigual-González, L. Gómez, J. Núñez, M. Vergara, A. Díaz-Barrera, J. Berrios, C. Altamirano, Application of a new model based on oxygen balance to determine the oxygen uptake rate in mammalian cell chemostat cultures, Chem. Eng. Sci. 152 (2016) 586–590, https://doi.org/10.1016/j.ces.2016.06.051.

[57] M. Aehle, A. Kuprijanov, S. Schaepe, R. Simutis, A. Lübbert, Simplified off-gas analyses in animal cell cultures for process monitoring and control purposes, Biotechnol. Lett. 33 (11) (2011) 2103, https://doi.org/10.1007/s10529-011-0686-5.

[58] J. Gálvez, M. Lecina, C. Solà, J.J. Cairó, F. Gòdia, Optimization of HEK-293S cell cultures for the production of adenoviral vectors in bioreactors using on-line OUR measurements, J. Biotechnol. 157 (1) (2012) 214–222, https://doi.org/10.1016/j.jbiotec.2011.11.007.

[59] A. Fontova, M. Lecina, J. López-Repullo, I. Martínez-Monge, P. Comas, R. Bragós, J.J. Cairó, A simplified implementation of the stationary liquid mass balance method for on-line OUR monitoring in animal cell cultures, J. Chem. Technol. Biotechnol. 93 (6) (2018) 1757–1766, https://doi.org/10.1002/jctb.5551.

[60] O. Henry, E. Dormond, M. Perrier, A. Kamen, Insights into adenoviral vector production kinetics in acoustic filter-based perfusion cultures, Biotechnol. Bioeng. 86 (7) (2004) 765–774, https://doi.org/10.1002/bit.20074.

[61] M. Rhiel, C.M. Mitchell-Logean, D.W. Murhammer, Comparison of Trichoplusia ni BTI-Tn-5B1-4 (high fiveTM) and Spodoptera frugiperda Sf-9 insect cell line metabolism in suspension cultures, Biotechnol. Bioeng. 55 (6) (1997) 909–920, https://doi.org/10.1002/(SICI)1097-0290(19970920)55:6<909::AID-BIT8>3.0.CO;2-K.

[62] A. Ghasemi, A. Bozorg, F. Rahmati, R. Mirhassani, S. Hosseininasab, Comprehensive study on wave bioreactor system to scale up the cultivation of and recombinant protein expression in baculovirus-infected insect cells, Biochem. Eng. J. 143 (2019) 121–130, https://doi.org/10.1016/j.bej.2018.12.011.

[63] G.W. Hiller, A.D. Aeschlimann, D.S. Clark, H.W. Blanch, A kinetic analysis of hybridoma growth and metabolism in continuous suspension culture on serum-free medium, Biotechnol. Bioeng. 38 (7) (1991) 733–741, https://doi.org/10.1002/bit.260380707.

[64] D.C.H. Jan, D.A. Petch, N. Huzel, M. Butler, The effect of dissolved oxygen on the metabolic profile of a murine hybridoma grown in serum-free medium in continuous culture, Biotechnol. Bioeng. 54 (2) (1997) 153–164, https://doi.org/10.1002/(SICI)1097-0290(19970420)54:2<153::AID-BIT7>3.0.CO;2-K.

[65] H.P.J. Bonarius, C.D. de Gooijer, J. Tramper, G. Schmid, Determination of the respiration quotient in mammalian cell culture in bicarbonate buffered media, Biotechnol. Bioeng. 45 (6) (1995) 524–535, https://doi.org/10.1002/bit.260450610.

[66] C. Zupke, G. Stephanopoulos, Intracellular flux analysis in hybridomas using mass balances and in vitro ^{13}C nmr, Biotechnol. Bioeng. 45 (4) (1995) 292–303, https://doi.org/10.1002/bit.260450403.

[67] K. Eyer, E. Heinzle, On-line estimation of viable cells in a hybridoma culture at various DO levels using ATP balancing and redox potential measurement, Biotechnol. Bioeng. 49 (3) (1996) 277–283, https://doi.org/10.1002/(SICI)1097-0290(19960205)49:3<277::AID-BIT5>3.0.CO;2-H.

[68] S.-J. Yoon, K.B. Konstantinov, Continuous, real-time monitoring of the oxygen uptake rate (OUR) in animal cell bioreactors, Biotechnol. Bioeng. 44 (8) (1994) 983–990, https://doi.org/10.1002/bit.260440815.

[69] O.T. Ramirez, R. Mutharasan, Cell cycle- and growth phase-dependent variations in size distribution, antibody productivity, and oxygen demand in hybridoma cultures, Biotechnol. Bioeng. 36 (8) (1990) 839–848, https://doi.org/10.1002/bit.260360814.

[70] A. Casablancas, X. Gámez, M. Lecina, C. Solà, J.J. Cairó, F. Gòdia, Comparison of control strategies for fed-batch culture of hybridoma cells based on on-line monitoring of oxygen uptake rate, optical cell density and glucose concentration, J. Chem. Technol. Biotechnol. 88 (9) (2013) 1680–1689, https://doi.org/10.1002/jctb.4019.

[71] G.A. King, A.J. Daugulis, P. Faulkner, M.F.A. Goosen, Recombinant β-Galactosidase production in serum-free medium by insect cells in a 14-L airlift bioreactor, Biotechnol. Prog. 8 (6) (1992) 567–571, https://doi.org/10.1021/bp00018a015.

[72] B. Maiorella, D. Inlow, A. Shauger, D. Harano, Large-scale insect cell-culture for recombinant protein production, Bio/Technol. 6 (12) (1988) 1406–1410, https://doi.org/10.1038/nbt1288-1406.

[73] L.A. Palomares, O.T. Ramirez, The effect of dissolved oxygen tension and the utility of oxygen uptake rate in insect cell culture, Cytotechnology 22 (1) (1996) 225–237, https://doi.org/10.1007/BF00353943.

[74] L.A. Palomares, S. Lopez, O.T. Ramirez, Utilization of oxygen uptake rate to assess the role of glucose and glutamine in the metabolism of infected insect cell cultures, Biochem. Eng. J. 19 (1) (2004) 87–93, https://doi.org/10.1016/j.bej.2003.12.002.

[75] T.K.K. Wong, L.K. Nielsen, P.F. Greenfield, S. Reid, Relationship between oxygen uptake rate and time of infection of Sf9 insect cells infected with a recombinant baculovirus, Cytotechnology 15 (1) (1994) 157–167, https://doi.org/10.1007/BF00762390.

[76] N. Kioukia, A. Nienow, A. Emery, M. Al-rubeai, Physiological and environmental factors affecting the growth of insect cells and infection with baculovirus, J. Biotechnol. 38 (3) (1995) 243–251, https://doi.org/10.1016/0168-1656(94)00128-Y.

[77] M. Lecina, A. Soley, J. Gràcia, E. Espunya, B. Lázaro, J. Cairó, F. Gòdia, Application of on-line OUR measurements to detect actions points to improve baculovirus-insect cell cultures in bioreactors, J. Biotechnol. 125 (3) (2006) 385–394, https://doi.org/10.1016/j.jbiotec.2006.03.014.

[78] B. Schopf, M. Howaldt, J. Bailey, DNA distribution and respiratory activity of Spodoptera frugiperda populations infected with wild-type and recombinant Autographa californica nuclear polyhedrosis virus (mammalian Cell Structure), J. Biotechnol. 15 (1) (1990) 169–185, https://doi.org/10.1016/0168-1656(90)90059-K.

[79] T. Gotoh, K. Chiba, K.-I. Kikuchi, Oxygen consumption profiles of Sf-9 insect cells and their culture at low temperature to circumvent oxygen starvation, Biochem. Eng. J. 17 (2) (2004) 71–78, https://doi.org/10.1016/S1369-703X(03)00140-2.

[80] S. Werner, J. Olownia, D. Egger, D. Eibl, An approach for scale-up of geometrically dissimilar orbitally shaken single-use bioreactors, Chem. Ing. Tech. 85 (1–2) (2013) 118–126, https://doi.org/10.1002/cite.201200153.

[81] K. Meier, W. Klöckner, B. Bonhage, E. Antonov, L. Regestein, J. Büchs, Correlation for the maximum oxygen transfer capacity in shake flasks for a wide range of operating conditions and for different culture media, Biochem. Eng. J. 109 (2016) 228–235, https://doi.org/10.1016/j.bej.2016.01.014.

[82] U. Maier, J. Büchs, Characterisation of the gas-liquid mass transfer in shaking bioreactors, Biochem. Eng. J. 7 (2) (2001) 99–106, https://doi.org/10.1016/S1369–703X(00)00107–8, special Issue: Shaking Bioreactors.

[83] X. Ni, S. Gao, R.H. Cumming, D.W. Pritchard, A comparative study of mass transfer in yeast for a batch pulsed baffled bioreactor and a stirred tank fermenter, Chem. Eng. Sci. 50 (13) (1995) 2127–2136, https://doi.org/10.1016/0009-2509(95)00050-F.

[84] R. Potumarthi, S. Ch, A. Jetty, Alkaline protease production by submerged fermentation in stirred tank reactor using Bacillus licheniformis NCIM-2042: Effect of aeration and agitation regimes, Biochem. Eng. J. 34 (2) (2007) 185–192, https://doi.org/10.1016/j.bej.2006.12.003.

[85] K. Van'T Riet, Review of measuring methods and results in nonviscous gas-liquid mass transfer in stirred vessels, Ind. Eng. Chem. Process Des. Dev. 18 (3) (1979) 357–364, https://doi.org/10.1021/i260071a001.

[86] M. Zlokarnik, Gas-Liquid Contacting. Stirring: Theory and Practice, John Wiley & Sons, Ltd,, 2001, pp. 126–205. Ch. 4.

[87] J.J. Chalmers, Mixing, aeration and cell damage, 30. years later: what we learned, how it affected the cell culture industry and what we would like to know more about, Curr. Opin. Chem. Eng. 10 (2015) 94–102, https://doi.org/10.1016/j.coche.2015.09.005.

[88] J.B. Sieck, W.E. Budach, Z. Suemeghy, C. Leist, T.K. Villiger, M. Morbidelli, M. Soos, Adaptation for survival: phenotype and transcriptome response of CHO cells to elevated stress induced by agitation and sparging, J. Biotechnol. 189 (2014) 94–103, https://doi.org/10.1016/j.jbiotec.2014.08.042.

[89] B. Neunstoecklin, T.K. Villiger, E. Lucas, M. Stettler, H. Broly, M. Morbidelli, M. Soos, Pilot-scale verification of maximum tolerable hydrodynamic stress for mammalian cell culture, Appl. Microbiol. Biotechnol. 100 (8) (2016) 3489–3498, https://doi.org/10.1007/s00253-015-7193-x.

[90] A.W. Nienow, W.H. Scott, C.J. Hewitt, C.R. Thomas, G. Lewis, A. Amanullah, R. Kiss, S.J. Meier, Scale-down studies for assessing the impact of different stress parameters on growth and product quality during animal cell culture (mixing), Chem. Eng. Res. Des. 91 (11) (2013) 2265–2274, https://doi.org/10.1016/j.cherd.2013.04.002.

[91] A.W. Nienow, The impact of fluid dynamic stress in stirred bioreactors - the scale of the biological entity: a personal view, Chem. Ing. Tech. 93 (1–2) (2021) 17–30, https://doi.org/10.1002/cite.202000176.

[92] A.W. Nienow, Reactor engineering in large scale animal cell culture, Cytotechnology 50 (1) (2006) 9, https://doi.org/10.1007/s10616-006-9005-8.

[93] J. Büchs, U. Maier, C. Milbradt, B. Zoels, Power consumption in shaking flasks on rotary shaking machines: I. Power consumption measurement in unbaffled flasks at low liquid viscosity, Biotechnol. Bioeng. 68 (6) (2000) 589–593, https://doi.org/10.1002/(SICI)1097-0290(20000620)68:6<589::AID-BIT1>3.0.CO;2-J.

[94] J. Büchs, U. Maier, C. Milbradt, B. Zoels, Power consumption in shaking flasks on rotary shaking machines: II. Nondimensional description of specific power consumption and flow regimes in unbaffled flasks at elevated liquid viscosity, Biotechnol. Bioeng. 68 (6) (2000) 594–601, https://doi.org/10.1002/(SICI)1097-0290(20000620)68:6<594::AID-BIT2>3.0.CO;2-U.

[95] C.P. Peter, Y. Suzuki, J. Büchs, Hydromechanical stress in shake flasks: correlation for the maximum local energy dissipation rate, Biotechnol. Bioeng. 93 (6) (2006) 1164–1176, https://doi.org/10.1002/bit.20827.

[96] W. Klöckner, C. Lattermann, F. Pursche, J. Büchs, S. Werner, D. Eibl, Time efficient way to calculate oxygen transfer areas and power input in cylindrical disposable shaken bioreactors. Biotechnol. Prog. 30 (6) (2014) 1441–1456, https://doi.org/10.1002/btpr.1977.

[97] P. Stephan, S. Kabelac, M. Kind, D. Mewes, K. Schaber, T. Wetzel (Eds.), VDI-Wärmeatlas, 12th edition, Springer Berlin Heidelberg, 2019, https://doi.org/10.1007/978-3-662-52989-8.

[98] E.A. Vogler, Structure and reactivity of water at biomaterial surfaces, Adv. Colloid Interface Sci. 74 (1) (1998) 69–117, https://doi.org/10.1016/S0001-8686(97)00040-7.

[99] F.R. Menter, Two-equation eddy-viscosity turbulence models for engineering applications, AIAA J. 32 (8) (1994) 1598–1605, https://doi.org/10.2514/3.12149.

[100] H. Kaufmann, X. Mazur, M. Fussenegger, J.E. Bailey, Influence of low temperature on productivity, proteome and protein phosphorylation of CHO cells, Biotechnol.

Bioeng. 63 (5) (1999) 573–582, https://doi.org/10.1002/(SICI)1097-0290(19990605)63:5<573::AID-BIT7>3.0.CO;2-Y.
[101] X. Mazur, H.M. Eppenberger, J.E. Bailey, M. Fussenegger, A novel autoregulated proliferation-controlled production process using recombinant CHO cells, Biotechnol. Bioeng. 65 (2) (1999) 144–150, https://doi.org/10.1002/(SICI)1097-0290(19991020)65:2<144::AID-BIT3>3.0.CO;2-Q.
[102] S.C. Kaiser, N. Perepelitsa, M. Kraume, D. Eibl, Development of the travelling wave bioreactor. Part II: engineering characteristics and cultivation results, Chem. Ing. Tech. 88 (1–2) (2016) 86–92, https://doi.org/10.1002/cite.201500091.
[103] C. Schirmer, T. Nussbaumer, R. Schöb, R. Pörtner, R. Eibl, D. Eibl, Development, engineering and biological characterization of stirred tank bioreactors, in: M.-K. Yeh, Y.-C. Chen (Eds.), Biopharmaceuticals, IntechOpen, Rijeka, 2018, https://doi.org/10.5772/intechopen.79444.
[104] Sartorius Stedim Biotech GmbH, User guide to MODDE 12 (2017).
[105] Pyles D., Brinegar C., Saville, M.A., Analysis of Kinematic Model Effects on SAR ECM, in: NAECON 2018 - IEEE National Aerospace and Electronics Conference, 2018, 309–317, doi:10.1109/NAECON.2018.8556649.
[106] G. van Rossum, Python 3.6.5 (2018). ⟨www.python.org⟩.
[107] A. Villiger-Oberbek, Y. Yang, W. Zhou, J. Yang, Development and application of a high-throughput platform for perfusion-based cell culture processes, J. Biotechnol. 212 (2015) 21–29, https://doi.org/10.1016/j.jbiotec.2015.06.428.